

Design of Graphene Based Conductive Blends

by

Mitasha SWAIN

THESIS PRESENTED TO ÉCOLE DE TECHNOLOGIE SUPÉRIEURE
IN PARTIAL FULFILLMENT FOR A MASTER'S DEGREE
WITH THESIS IN MECHANICAL ENGINEERING
M.A.Sc.

MONTREAL, JANUARY 19, 2021

ÉCOLE DE TECHNOLOGIE SUPÉRIEURE
UNIVERSITÉ DU QUÉBEC



Mitasha SWAIN, 2020



This Creative Commons licence allows readers to download this work and share it with others as long as the author is credited. The content of this work can't be modified in any way or used commercially.

BOARD OF EXAMINERS

THIS THESIS HAS BEEN EVALUATED
BY THE FOLLOWING BOARD OF EXAMINERS

Mrs Nicole R. Demarquette, Thesis Supervisor
Department of Mechanical Engineering at École de technologie supérieure

Mr. Eric David, President of the Board of Examiners
Department of Mechanical Engineering at École de technologie supérieure

Mrs. Emna Helal, Member of the jury
NanoXplore Inc.

Mr. Philippe Bocher, Member of the jury
Department of Mechanical Engineering at École de technologie supérieure

THIS THESIS WAS PRESENTED AND DEFENDED
IN THE PRESENCE OF A BOARD OF EXAMINERS AND PUBLIC
DECEMBER 17, 2020
AT ÉCOLE DE TECHNOLOGIE SUPÉRIEURE

ACKNOWLEDGEMENTS

First, I would like to express my best sincere gratitude to my research supervisor Dr. Nicole R. DEMARQUETTE for this opportunity and it is through the quality of her guidance, encouraging my ideas, financial support and her patience throughout my project. I am really grateful for her constant guidance and the time which she invested in my project which really means a lot to me.

I would also like to thank Prof Eric David from ETS and Mrs Emna Helal for accepting to examine this work and be a part of member of the jury.

Also a special thanks to MITACS, ETS and NSERC for the financial support of my project.

I would also like to particularly thank the technicians for their help to work safely in the laboratory, Simon Laflamme for taking my very first SEM picture with me and Nabil Mazeghrane for the use of mini extruder, press machine and big extruder and Radu Romanica for the use of Thermo Gravimetric Analysis. Obviously, I would also like to the students present during my stay at ETS in Montreal: Emna, Rafael, Julie, Nourin, Daria, Jose, Camila, Chloe, Marwa, Rihab and Manon.

I would particularly like to thank the people whom I got to know better outside. Nourin and Daria for her constant support and constantly motivating me to do better and for lots of conversations during lunch. Rihab with whom I spent some very good moments roaming in parks around the city during this lockdown and lots of conversation. Special thanks to all my colleagues for the knowledge they passed on to me and I wish for them excellent continuity of their theses.

A special thanks to my roommates: Ashish and Rhythm for their constant encouragement throughout my thesis and cheering me up during my difficult times and always being there by my side and their constant care and motivation without whom this work would not have been possible and also my friends: Aashima, Ajin, Nisha, Shikha, Arna, Aryan, Siva, Rishi and Hayati for making my stay in Montreal memorable.

Finally , I would like to thank my parents and sister: Nikita and brother in law: Achyut and all my family members for their support and for instilling in me a sense of work ethic and always pushing me to do my best without which this work would not have been possible.

Conception de mélanges conductifs à base de graphène

Mitasha SWAIN

RÉSUMÉ

Dans ce travail, l'effet de la taille des nanoparticules de graphène (GnP) sur le comportement électrique et rhéologique des polymères purs et des mélanges co-continus a été évalué. Deux types de graphène présentant pour l'un, une surface spécifique de 750 m²/g, et pour l'autre, une surface spécifique de 50-80 m²/g ont chacun été mélangé dans des concentrations variant de 1 à 10% en poids avec le polyméthylméthacrylate (PMMA), ou avec du polystyrène (PS), ou enfin avec un mélange 50/50 de PMMA/PS. Les matériaux ont été obtenus par extrudeuse à deux vis. De plus, les mélanges ont été recuits à 200 ° C pendant 30 minutes, 1 heure et 2 heures sous une pression de 0,8 MPa dans la presse hydraulique. La morphologie et les propriétés électriques du matériau avant et après recuit ont été évaluées par microscopie électronique à balayage et par spectroscopie diélectrique à large bande. Il a été montré que le PMMA présentait un seuil de percolation inférieur à celui du PS et que l'utilisation d'un mélange de polymère pouvait réduire le seuil de percolation. De plus, les résultats ont indiqué que le seuil de percolation était plus bas pour les mélanges avec des nanoparticules de graphène ayant une plus grande surface. Il a également été montré que les nanoparticules de graphène ayant une surface spécifique élevée migrent plus rapidement vers la phase plus favorable que les nanoparticules de graphène ayant une surface spécifique inférieure affectant ainsi les propriétés électriques et rhéologiques. La taille des nanoparticules de graphène affecte la redistribution des nanoparticules de graphène dans la formation du réseau co-continu et le module de conservation du mélange.

Mots-clés: nanoparticules de graphène, surface de contact, mélanges co-continus, effet de taille, recuit thermique, seuil de percolation, interfaces, conductivité électrique, module de conservation.

Design of Graphene Based Conductive Blends

Mitasha SWAIN

ABSTRACT

In this work, the effect of graphene platelet size on the electrical and rheological behavior of pure polymers and co-continuous blends was evaluated. Graphene presenting a surface area of 750 m²/g and a surface area of 50-80 m²/g was added in concentrations varying from 1 to 10 weight% to polymethylmethacrylate (PMMA), polystyrene (PS) and 50/50 PMMA/PS blend. The materials were obtained by twin screw extruder. The blends were further annealed at 200°C for 30 minutes, 1 hour and 2 hours under a pressure of 0.8 MPa in the hydraulic press. The morphology and electrical properties of the material prior and after annealing were evaluated by scanning electron microscopy and by broadband dielectric spectroscopy. It was shown that PMMA presented a lower percolation threshold than PS and that using a blend could reduce the percolation threshold. It was also shown that using blends is an interesting method to reduce the percolation threshold. Furthermore, the results indicated that the percolation threshold was lower for blends filled with graphene nanoplatelets having a larger surface area. It was also shown that graphene nanoplatelets having high surface area migrate faster towards the more favorable phase than the graphene nanoplatelets having lower surface area thus affecting the electrical and rheological properties. The size of graphene nanoplatelets affect the redistribution of the graphene nanoplatelets in the formation of co-continuous network and strength of the blend matrix.

Key Words: graphene nanoplatelets, surface area, co-continuous blends, size effect, thermal annealing, percolation threshold, interfaces, electrical conductivity, storage modulus.

TABLE OF CONTENTS

	Page
INTRODUCTION.....	1
CHAPTER 1 LITERATURE REVIEW.....	7
1.1. Chapter Outline.....	7
1.2. Conductive polymer systems.....	7
1.2.1. Introduction.....	7
1.2.2. Intrinsically Conducting Polymers.....	7
1.2.3. Conductive filled nanocomposites.....	8
1.2.3.1. Conducting Nanoparticles.....	9
1.2.3.2. Percolation Threshold.....	11
1.2.3.3. Control of nanocomposites properties.....	12
1.3. Polymer blends.....	14
1.3.1. Definition.....	14
1.3.2. Factors that affect the morphology of polymer blends.....	15
1.4. Conductive polymer blends.....	19
CHAPTER 2 OBJECTIVES.....	25
CHAPTER 3 EXPERIMENTAL.....	27
3.1. Choice of materials.....	27
3.1.1. PS.....	27
3.1.2. PMMA.....	27
3.1.3. Graphene nanoplatelets.....	28
3.1.3.1. Characteristics of graphene nanoplatelets.....	28
3.2. Methodology.....	29
3.2.1. Processing Methods.....	29
3.2.2. Rheological Properties.....	29
3.2.3. Electrical Properties.....	30
3.2.4. Morphology Characterization.....	31
CHAPTER 4 RESULTS AND DISCUSSIONS.....	33
4.1. Analysis of wetting coefficient theory for PS/PMMA blend.....	33
4.2. Analysis of the diffusion of GNPs in the polymer systems.....	34
4.3. Influence of adding graphene nanoplatelets on the pure phases.....	33
4.3.1. Results.....	35
4.3.2. Discussions.....	39
4.3.2.1. Concentration of the graphene nanoplatelets.....	39
4.3.2.2. Polymer Matrix.....	40
4.3.2.3. Size of the graphene nanoplatelets.....	41
4.4. Use of blend to decrease the percolation threshold of the materials.....	43
4.4.1. Choice of concentration for polymer blend.....	43

4.4.1.1.	Results	45
4.4.1.2.	Discussions	51
4.4.1.2.1	Concentration of the graphene nanoplatelets	51
4.4.1.2.2	Masterbatch used	52
4.4.1.2.3	Size of the graphene nanoplatelets	53
4.5.	Correlation between electrical and rheological percolation.....	55
4.6.	Effect of annealing on the blends.....	56
4.6.1.	Results	57
4.6.1.1.	Electrical Characterization of annealed blends	57
4.6.1.2.	Time Sweep Tests.....	59
4.6.1.3.	Effect of annealing on blend morphology.....	61
CONCLUSIONS.....		65
BIBLIOGRAPHY.....		67

LIST OF TABLES

		Page
Table 1.1	Values of conductivity of the ICPs.....	8
Table 1.2	Properties of graphene nanoplatelets	9
Table 1.3	Comparison of the properties of GNPs.....	10
Table 1.4	Comparison of metallic nanoparticles with graphene.....	10
Table.1.5	Equilibrium condition for selective localization of GNPs.....	20
Table 3.1	Properties of Polystyrene (PS).....	27
Table 3.2	Properties of Polymethylmethacrylate (PMMA).....	28
Table 3.3	Specifications of different grades of graphene used in this project.....	28
Table 4.1	Surface tension of the materials.....	34
Table 4.2	Rotary Diffusivity and the rate of migration of the different grades of GNPs in the polymers.....	35
Table 4.3	Slope analysis of log G' vs log ω at lower frequencies (0.01-0.08 rad/s).....	37
Table 4.4	Slope analysis of log G' vs log ω at lower frequencies (0.01 - 0.08 rad/s) for filled PMMA phases.....	38
Table 4.5	Slope analysis of log G' vs log ω at lower frequencies (0.01 -0.08 rad/s) for PS based blends filled with Graphene Grade C and Grade H.....	47
Table 4.6	Slope analysis of log G' vs log ω at lower frequencies (0.01 -0.08 rad/s) for PMMA based blends filled with Graphene Grade C and Grade H.....	49

LIST OF FIGURES

		Page
Figure 4.1	Electrical Conductivity as a function of concentration of GNPs for a)filled PS phases b)filled PMMA phases.....	36
Figure 4.2	Storage modulus as a function of angular frequency for a)PS filled with grade C b)PS filled with grade H	37
Figure 4.3	Storage modulus as a function of angular frequency for PMMA filled with grade C b)PMMA filled with grade H	38
Figure 4.4	Viscosity vs shear rate for pure polymer phases (PS & PMMA) and filled polymer phases (PS and PMMA)	44
Figure 4.5	Micrographs of neat blends (PS/PMMA)in the ratio of (30/70).....	44
Figure 4.6	Micrographs of neat blends (PS/PMMA) in the ratio of (50/50)	45
Figure 4.7	Electrical Conductivity as a function of concentration of <i>GNPs</i> for a)PS based blends b)PMMA based blends where PS/PMMA is in the ratio of 50/50.....	46
Figure 4.8	Storage Modulus as a function of angular frequency for PS based blends filled with GNPs a)Grade C and b)GradeH.....	47
Figure 4.9	Storage Modulus as a function of angular frequency for PMMA based blends filled with Graphene a)Grade C and b) Grade H.....	48
Figure 4.10	Micrographs of a) neat PS/PMMA b)PS/PMMA/Graphene Grade C_PMMA_MB c) PS/PMMA/Graphene Grade H_PMMA_MB with ratio of PS/PMMA as 50/50.....	50
Figure 4.11	Rheological percolation taken at 0.01 rad/s as a function of graphene concentration for different composites prepared from a)PSMBb)PMMAMB.....	56
Figure 4.12	Conductivity as a function of concentration of graphene nanoplatelets for annealed blends fabricated from a)PS Masterbatch filled with	

Graphene Grade C b)PS Masterbatch filled with Graphene Grade H
 c)PMMA Masterbatch filled with Graphene Grade C d)PMMA
 Masterbatch filled with Graphene Grade H
59

Figure 4.13 Storage modulus as a function of annealing time for blends fabricated
 from a)PS Masterbatch filled with Graphene Grade C b)PS Masterbatch
 filled with Graphene Grade H c)PMMA Masterbatch filled with
 Graphene Grade C d)PMMA
 Masterbatch filled with Graphene Grade H61

Figure 4.14 Morphology of blends fabricated from a)PMMA Masterbatch filled with
 Graphene Grade C before annealing b)PMMA Masterbatch filled with
 Graphene Grade C after annealing c)PMMA Masterbatch filled with
 Graphene Grade H before annealing d)PMMA Masterbatch filled with
 Graphene Grade H after annealing for 60 minutes at 200°C.
63

LIST OF ABBREVIATIONS

CNTs	Carbon Nanotubes
EVA	Ethylene-Vinyl Acetate
GNPs	Graphene Nanoplatelets
LLDPEs	Linear Low Density Polyethylene
MWNTs	MultiWalled Nanotubes
PLA	PolyLactic Acid
PMMA	Polymethylmethacrylate
PS	Polystyrene
PVDF	PolyVinylidene Fluoride

INTRODUCTION

Polymers are generally insulating in nature. However, a few intrinsic conducting polymers (ICPs) are in existence which have conjugated bonds along the polymer backbone which help in the mobility of the electrons rendering the polymers conducting. These ICPs have their electrical conductivity value around the range of 10^5 S/cm attracting the attention of various researchers and have become the subject of intense research. These polymers are more and more involved in a wide range of applications like sensors, thin film transistors, rechargeable batteries, solar cells, light emitting diodes (LEDs), supercapacitors, electrochromic devices (Ates et al., 2012) electromagnetic shielding devices, printed electronic circuits (Kumar et al., 2015), memory devices, imaging materials (Ziadan, 2012). Owing to their outstanding properties like cheap cost, light weight, environmental and thermal stability, corrosion resistance, these materials have been always a subject of intense research. But despite the advantages, these materials also have some disadvantages which cannot be neglected. These ICPs are rigid along the polymer chains because of the conjugated bonds as a result of which they are insoluble or infusible (Ramakrishnan, 1997) making their processing difficult. There are various alternatives to render conducting polymers. One of the alternative ways of fabricating polymer systems is by the inclusion of conductive nanofillers in the insulating polymers (Koncar, 2019).

Carbon-based nanofillers (carbon black, graphene nanoplatelets, carbon nanotubes, graphene oxide) and metallic nanofillers are the fillers that can be added in order to increase the conductivity of the polymer systems (Thomas et al., 2016). Though the metallic nanofillers have higher conductivity value than the carbon-based nanofillers, the metallic nanofillers get oxidized forming an insulating layer on the surface which leaves us with the carbon based nanofiller as the only option for the fillers in the polymer systems. Recently, graphene amongst the carbon-based nanofillers has been attracting the attention of the researchers as a potential filler to enhance the electrical conductivity of the matrix owing to its remarkable properties like light weight, low density, low cost, high aspect ratio, remarkable electrical conductivity, planar structure, high effective surface area (Cataldi et al., 2018). Graphene based composites

have been attracting the attention of the researchers and they are being used in various fields like sensors, automobile components, conductive inks, biomedicines, solar cells, membranes (Mohan et al., 2018) and many other fields.

The main and the foremost goal of this project is to design an electrically conductive polymer system. So, the characteristic which we are mainly focusing on is electrical conductivity of the polymer systems. Electrical conductivity in these polymer systems is closely associated with the formation of a continuous conductive network in the matrix (Huang, 2002). In the polymer systems filled by the conductive nanoparticles, the continuous conductive network is a continuous pathway formed by the conductive nanoparticles. Therefore, conductivity depends on the filler concentration, aspect ratio of the fillers, polymer-filler interactions, crystallinity of the polymers and also on the dispersion of conductive fillers in the matrix.

One of the factors which should also be taken into consideration is the cost of the material being fabricated. A material is always designed keeping the cost of fabrication as low as possible. The cost of such conductive polymer systems can be optimized by optimizing the filler concentration without compromising the electrical and mechanical properties. In general, the conductive polymer systems composed of single polymer require a substantial amount of filler to form a continuous conductive network around the whole polymer matrix thereby increasing the cost of the system as well as the melt viscosity. (Brigandi et al., 2014) The only way by which the filler concentration can be optimized retaining the appropriate electrical and mechanical properties is by the use of multiphase structures composed of immiscible polymers.

Properties of multiphase structures depend on various factors like properties of individual components, adhesion between the components and the blend morphology which in turn is dictated by the interfacial tension (Pötschke & Paul, 2003). When two immiscible polymers are blended, there are basically two types of blend morphologies which are often observed: co-continuous and droplet-in-matrix morphology (Jianming Li et al., 2002). There are several factors which affect the evolution of morphology of the blend during compounding like temperature of compounding, duration of mixing in the compounder, viscosity ratio, blend composition, intensity of compounding (screw speed) (Lee & Han, 1999), interfacial tension.

A co-continuous structure is just a thermodynamic nonequilibrium state which exists only at phase inversion when one mode of droplet-in-matrix morphology to the other mode of droplet-in-matrix morphology with increase in the content of dispersed phase. Considering a droplet-in-matrix morphology to be conductive, in order to form a continuous network of fillers, the concentration of fillers to be added is generally higher than in case of co-continuous morphology. And since the filler concentration should be optimized, blend morphology must be co-continuous. In case of blends, the optimal filler concentration (also known as percolation threshold) also depends on the size of the fillers (Wang et al., 2015) which has not been studied by many researchers.

The next most important step in the fabrication of conductive polymer composites is selective localization of the nanoparticles in the polymer blends. Selective localization of the nanoparticles in the polymer blends is a very important factor since the interfacial nanoparticles control the morphology and help in reducing the percolation threshold (You & Yu, 2018) and the nanoparticles if present in one phase may agglomerate increasing the melt viscosity of the system thereby making the processing difficult. and selective localization of nanoparticles in the polymer blends is a very crucial step during the fabrication of high performance, functional and responsive materials (Brigandi, 2017).

Another method by which the percolation threshold can be optimized is by the use of post-processing treatments like thermal annealing. In general, when the fillers form a conductive network in the polymer matrix, these fillers are usually in a thermodynamic non-equilibrium state and these fillers may rearrange themselves over time when subjected to an annealing temperature which is higher than the melting temperature of the polymer matrix or softening temperature in general. This mechanism is known as the dynamic percolation. These particles during annealing may migrate and rearrange themselves to form a better continuous conductive network increasing the electrical conductivity of the system. But the rate at which the nanoparticles migrate towards the interface is influenced by the shape factor of the nanoparticles and also the viscosity of the polymer matrix. According to Slim Fast Mechanism, the particles with large aspect ratio migrate faster than the particles with low aspect ratio. So, the rearrangements of the nanoparticles are influenced by the size of the nanoparticles.

(Salehiyan & Ray, 2019) These rearrangements may also induce some changes in the morphology of the blends and the conductive nanoparticles may migrate towards the interface in due course of time thereby reducing the percolation threshold.

A previous study has been done in our group which showed that conductive polymer system with co-continuous blend morphology was possible for EVA/HDPE with a commercial Graphene nanoplatelets. The polymers were semi crystalline in this study and the effect of crystallinity was also studied (Emna Helal et al., 2019). But the effect of platelet size was not studied. Hence, in order to reduce the complication factors, a blend of amorphous polymers was selected for our study.

In this study, co-continuous blends of two amorphous polymers, polystyrene (PS) and polymethylmethacrylate (PMMA) filled with commercial graphene nanoplatelets having different platelet size are studied. These blends have been fabricated by melt blending technique. In this study, the effect of the size of graphene nanoplatelets have been investigated on the characteristics of the filled polymer blends. PS and PMMA have been chosen as the polymers since they form a model polymer blend and since they are amorphous, the impact of crystallinity of the polymers can be ruled out.

In view of the points considered above, the objectives can be very well stated at present. The present study emphasizes on the size effect of the graphene nanoplatelets on the evolution of the electrical conductivity, rheological behavior and the microstructure in PS/PMMA/GNPs materials and it also focuses on the evolution of the properties during thermal annealing.

This thesis aims at expanding our knowledge on the polymer blends filled with nanoparticles with different sizes and their electrical and rheological behavior. Chapter 2 presents the literature review investigating basics of conductive polymer systems, conducting particles present in nature which can be used as fillers in conductive polymer systems and the factors affecting the rheological, electrical behavior and the morphology of the conducting polymer systems. Chapter 3 clearly details the primary as well as the secondary objectives of the study. Chapter 4 presents the choice of the polymers used in the study and the specification of different sized nanoparticles used as fillers and it also clearly details out the experimental

methodologies used for the design of the polymer system and characterization of different properties of the polymer systems. Chapter 5 presents the results and discussions of the study. The electrical and rheological behavior of the PS/PMMA blends to which the graphene nanoplatelets were added were greatly influenced by the size of the graphene nanoplatelets, their selective localization and thermal annealing.

CHAPTER 1

LITERATURE REVIEW

1.1. Chapter Outline

After a brief introduction, the different types of conductive polymers will be introduced. In particular, the advantages of nanocomposites comprising conductive nanoparticles over the intrinsically conductive polymers will be highlighted. The different types of nanoparticles that can be added to the dielectric polymers will be presented. The first part helps us in understanding the reason behind the usage of polymer blends in order to obtain the conductive nanocomposites. The second part will present the fundamentals of polymer blends. Finally, the state of art of conductive polymer blends will be presented.

1.2. Conductive polymer systems

1.2.1. Introduction

In general, polymers are intrinsically dielectric or in other words, we can call them insulating. However, under certain circumstances, these polymers can conduct electricity. This is true for intrinsically conducting polymers and composites containing conductive particles. The above-mentioned materials are presented below

1.2.2. Intrinsically Conducting Polymers

There are various intrinsically conducting polymers like polyacetylene, polypyrrole, polythiophene, polyaniline, poly (phenyl vinylene) (Y. Li et al., 2010). These polymers have a conjugated structure which helps them to behave as semiconductors by decreasing the band gap between the valence band and conduction band.

Intrinsically conducting polymers have mobile electrons to participate in the electron transport which enhances their conducting nature.. When electrons are added or removed in the valence or conduction bands via the doping mechanism, the conducting polymers present a conductivity that ranges from 10^2 - 10^5 S/cm. The conductivity values of some of the intrinsically conducting polymers are stated in Table 1.1 .(Database, 2017)

Table 1.1 Values of conductivity of the intrinsically conducting polymers
Adapted from Polymer Properties Database,2017

Conducting Polymers	Conductivity (S/cm)
Polyacetylene	$10^3 - 10^5$
Polythiophene	10^3
Polypyrrole	$10^2 - 7.5 \cdot 10^3$
Poly (p-phenylene)	$10^2 - 10^3$
Polyaniline	$2 \cdot 10^2$
Poly (p-phenylene vinylene)	$2 \cdot 10^4$

Unfortunately, intrinsically conducting polymers are difficult to process (Dogan et al., 2010) and are costly and are insoluble in most solvents (Hatchett & Josowicz, 2008). This is one of the reasons why, engineers or researchers are preferring the development of blends or composites containing conductive nanoparticles which will confer electrical conductivity to normally electrically non-conductive polymers.

1.2.3. Conductive filled nanocomposites

As we have already discussed above, polymers can be made conducting by filling the insulating polymers with conductive particles. This method is a very cost-efficient method as compared to the use of intrinsically conducting polymers. The electrical properties of the insulating polymers can be modified considerably by the introduction of conducting particles in the insulating polymers. In this work, only nanoparticles will be considered. and below, characteristics of nanoparticles that can be added to insulating polymers to turn them electrically conductive are reviewed. After the concept of percolation threshold, which corresponds to the concentration of nanoparticles at which the composite starts to conduct electricity is presented. Then, it will be shown how important it is to control the morphology of the composites in order to control their properties.

1.2.3.1. Conducting Nanoparticles

Nanoparticles are particles which present one of their dimensions in the range of 1 to 100 nm. These nanoparticles have varied range of shapes like platelets, spheres, rods, tubes, cages, shells depending on the number of dimensions of the particles which are nanosized. The nanoparticles used are of great importance since there is a significant change in the physicochemical properties of the particles with varying size.

There are various types of nanoparticles which have been used till date. To name just a few, they are carbon nanotubes, graphene nanoplatelets, fullerenes, copper, gold, silver nanoparticles and many more. But, in view of the objectives of our project, we will be using graphene nanoplatelets which have been recently discovered

The discovery of graphene nanoplatelets can be traced back to the 15th century when pencil was first discovered by Simono and Lyndiana Bernacotti. This was followed by exploration into the structure of graphite by John Desmond Bernal in the 19th century (Canada, 2015). Professor Andre Geim and Professor Kostya Novoselov finally succeeded in isolating graphene single layers from graphite by Scotch Tape method in 2004. Graphene nanoplatelets are known for their excellent mechanical properties (flexibility, strength and surface hardness), superb electrical and thermal properties (STREM) which are well illustrated in Table 1.2. The values of the properties are mentioned for single layer graphene nanoplatelets

Table 1.2 Properties of graphene nanoplatelets
Adapted from Strem Chemicals Inc (STREM)

Property	Value
Electrical Conductivity	10^7 S/m
Tensile Strength	5 GPa
Tensile modulus	1000 GPa
Thermal Conductivity	3000 W/mK
Thermal Expansion	$4-6 \cdot 10^{-6}$ /K

Graphene nanoplatelets can also be cheaper than the other conductive nanoparticles (carbon nanotubes or metallic nanoparticles) which is well illustrated in Table 1.3

Table 1.3 Comparison of the properties of GNPs with that of CNTs
Adapted from Strem Chemicals Inc (STREM) and Y.Wang et al (Wang & Weng, 2018)

Properties	Values of Graphene Nanoplatelets	Values of carbon nanotubes
Lateral size	Up to 50 microns	Average diameter= 0.83 nm
Electrical Conductivity	10^7 S/m	10^6 S/m
Bulk density	0.2-0.4 g/cc	0.1 g/cc
Price	203 Can\$/250 g (ALDRICH)	1125Can\$/1g (ALDRICH)

Thus, the primary objectives of obtaining conductive polymer systems at the lowest cost possible can be fulfilled by using Graphene nanoplatelets.

Table 1.4 Comparison of metallic nanoparticles with graphene nanoplatelets
Adapted from Y. Wang et al (Wang & Weng, 2018)

Property	Silver nanoparticles	Copper nanoparticles	Graphene nanoplatelets
Conductivity	$6.3 \cdot 10^7$ S/m	$5.96 \cdot 10^7$ S/m	10^7 S/m
Price	188.50 Can\$/5 g (ALDRICH)	92.30 Can\$/ 25g (ALDRICH)	203 Can\$/250 g

Graphene has found its applicability in various fields like electrodes (Zhang et al., 2009), graphene inks (Hatchett & Josowicz, 2008), tough screen displays (Li et al., 2010), photodetectors (Ates et al., 2012), inkjet-printed graphene electronics (Ziadan, 2012), batteries electrodes (Brigandi et al., 2014), sensors (Kumar et al., 2015), cars and aircrafts (Flagship,

2017) and they have proved to be more promising candidates in terms of cost and quality when compared with single layer graphite. Therefore, in view of the objectives of our project, we shall be using graphene nanoplatelets as fillers in the nanocomposites for inducing conductivity in the composites which will be discussed in the next sections.

1.2.3.2. Percolation Threshold

Electrical conductivity in conductive filled nanocomposites can be well described by the percolation theory (Mutlay & Tudoran, 2014) which states that there is a minimum concentration of the nanoparticles below which the fillers are isolated in the insulating matrix, termed as the percolation threshold. If one increases the concentration of the nanoparticles beyond the percolation threshold, the interconnection between the particles increases and hence is the probability of formation of a continuous conductive network. The formation of a continuous conductive network is related to the sharp increase in the value of conductivity at a critical concentration known as the percolation threshold.. But there is a critical value beyond which if the concentration of nanoparticles is increased, the nanoparticles agglomerate which leads to the increase in the viscosity of the system which complicates the processing of the system. Hence, this fact emphasizes on the point that the amount of the conductive inclusions should be minimized in order to lower the cost of the whole system. Percolation threshold can be related to the aspect ratio of the nanoparticles depending on the structure of the nanoparticles. But, the percolation threshold for the graphene nanoplatelets having sheet like structure have a different co-relation with the aspect ratio. The percolation threshold unlike for the other nanoparticles have an inverse relation with the aspect ratio for graphene nanoplatelets. There are various models describing the relationship between the percolation threshold and the aspect ratio like:

For isotropically oriented discs, the percolation threshold was related to the aspect ratio by the following Equation 1.1:

$$\phi^c = 1.46 * \frac{1}{\alpha} \quad (1.1)$$

(where ϕ_c refers to the percolation threshold and α refers to the aspect ratio of the nanoparticles)

Li and Kim (Jing Li & Kim, 2007) developed a relationship between the percolation threshold and the geometry of the graphene nanoplatelets and their distribution which is prevalent from the Equation 1.2:

$$\phi_c^{2D} = \frac{2\pi D^2 t}{(D + \xi)^3} \quad (1.2)$$

Where ϕ_c refers to the percolation threshold of the graphene nanoplatelets, D is the diameter of the graphene nanoplatelets, t is the thickness of the graphene nanoplatelets and ξ refers to the distance between the graphene nanoplatelets

1.2.3.3. Control of nanocomposites properties.

The performance of the polymer nanocomposites refers to the effectiveness of the polymer nanocomposites with respect to various parameters like electrical properties, mechanical properties and the like. Performance of the polymer nanocomposites depend on a number of factors like the fillers used, structure of the fillers, concentration of the fillers and the other factors are mentioned in the successive lines. The structural differences between the fillers in the polymer nanocomposites can have a significant impact on the performance of the polymer nanocomposites. Some of the factors which affect the performance of the polymer nanocomposites can be stated as the processing methods, post production techniques and it also includes the different types of fillers (Marsden et al., 2018)

For example, in case of carbon filled polymer nanocomposites, carbon nanotubes and the graphene nanoplatelets both have synergetic effect and aids in yielding polymer nanocomposites which have better efficiency than when filled with individual components (Kuester, 2017).

In conclusion, there is a direct relation between the processing and performance of the polymer nanocomposites. The processing methodology is a crucial factor in determining the performance of the polymer nanocomposites. In past years, the solution-based techniques used

for fabricating reduced graphene filled polymer nanocomposites yielded materials with less conductivity. But, in recent years, this field has seen a huge improvement with recent exploration of various fabrication techniques like liquid exfoliation techniques which do not require functionalizing the graphene nanoplatelets. The fillers produced by this technique have high intrinsic conductivity and are produced in large volumes and therefore used for enhancing the performance of the polymer nanocomposites.

The filled single-phase polymers consisting of conductive fillers such as carbon nanotubes, carbon black or graphene nanoplatelets have been used in a wide range of applications ranging from antistatic and electrostatic dissipation materials to the utility in electromagnetic shielding materials (Brigandi et al., 2014).

But the filled single-phase polymers require a considerable amount of conductive fillers in order to have a continuous network of conductive fillers and enhance the conductivity up to a range of only 10^{-7} S/m – 10^{-4} S/m. But as mentioned before, the increase in the amount of conductive fillers increases the viscosity of the whole system thereby making the processing of the composites difficult and it also decreases the mechanical and rheological properties of the nanocomposites. The increase in the amount of nanofillers increases the probability of agglomeration of the conductive nanofillers thereby disrupting the uniform dispersion of the conductive nanofillers. The problem of uniform dispersion of the conductive fillers in the nanocomposites still remains as a challenge which needs to be solved by the researchers and the researchers need to get it solved at the lowest cost possible. Surfactants can be used to minimize the agglomeration of the conductive nanofillers in the nanocomposites but the use of surfactants tends to increase the cost of the nanocomposites. One of the examples which clearly states the problem mentioned above and how the researchers tried to solve the problems and what were the new problems which they had to face is mentioned in the next paragraph.

C. Zhang et al (Zhang et al., 2009) studied the effect of filler content on the conductivity and the percolation threshold for a system of PVDF and Multiwalled Carbon Nanotubes (MWNTs). They also tried to improve the dispersion of the multiwalled carbon nanotubes in PVDF by treating MWCNTs with carboxylic acid and found that even if the carbon nanotubes were well

dispersed, the percolation time and the activation energy of the system was higher than the PVDF/MWNTs implying that the former system is less stable than the latter system. The surface modification of the carbon nanotubes had a stronger interaction with the polymer which tends to increase the percolation time owing to the decrease of the mobility of the system.

So, the alternative solution for maintaining a uniform dispersion of the conductive nanofillers at the lowest cost possible can be through the utilization of polymer blends which we shall be discussing in the next section.

1.3. Polymer blends

1.3.1. Definition

A polymer blend can be well defined as a mixture of two or more polymers in which the concentration of each of the constituent must be above 2 weight%. (Utracki, 1999) Blends are either miscible, partially miscible or immiscible. The miscibility of the polymer blends can be determined from the free energy of mixing. The free energy of mixing can be described by the Equation 1.3:

$$\Delta G_m = \Delta H_m - T\Delta S_m \quad (1.3)$$

Where ΔG_m represents the free energy of mixing, ΔH_m represents the enthalpy of mixing, T represents the temperature at which the processing is taking place and ΔS_m represents the entropy of mixing.

But in view of the objectives of our project, we want benefit from the multiphase morphology which can be accomplished by using an immiscible blend. In the case of immiscible blends, there are several factors that have an impact on the obtained morphology which are presented below

1.3.2. Factors that affect the morphology of polymer blends

Immiscible polymer blends have varying morphologies like droplet in a matrix morphology, co-continuous morphology, fiber morphology and laminar morphology. The different types of morphology are influenced by the processing conditions, compositions of the blend. The morphology which is of interest to us in this project is the co-continuous morphology. Co-continuous morphology comprises of a multi-phase polymer blend in which each of the polymers form a continuous network. A low volume fraction of the dispersed polymer phase results in the formation of a droplet-in-matrix morphology. As the volume fraction of the dispersed phase increases, the droplet-in-matrix morphology converts into a co-continuous morphology but the co-continuous morphology is not stable so, increase in the volume fraction of the dispersed component beyond a certain value results in the formation of droplet-in-matrix morphology with the minor phase forming a continuous phase. There is a very narrow range within which the co-continuous morphology exists and the composition at which droplet-in-matrix changes into co-continuous morphology is given by the equation 1.4 developed by Paul and Barlow (Paul & Barlow, 1980)

$$\frac{\eta(\gamma_1)}{\eta(\gamma_2)} = \frac{\phi_1}{\phi_2} \quad (1.4)$$

Where η refers to the viscosity and ϕ refers to the volume fraction of the constituents in the polymer blends. There are other models which describe the influence of various parameters on the phase inversion (conversion of droplet-in-matrix morphology to co-continuous morphology).

There are various other factors which affects the morphology like annealing, fillers and the like. We will not be describing in details the effects of all the concerning factors on morphology but will go into a detailed description of the influence of annealing and the effect of introducing fillers on the morphology of the immiscible polymer blends

As mentioned above, the co-continuous morphology is thermodynamically unstable whereas droplet-in-matrix morphology is a more thermodynamically stable morphology. In a due course of time, the phase size increases with a reduction in the interfacial area which can be termed as coarsening of the phases. The coarsening of the phases occurs both in droplet-in-matrix morphology and co-continuous morphology. In case of droplet-in-matrix morphology, coarsening occurs by the coalescence of the phases and in case of co-continuous morphology, coarsening occurs by the breakup and dissolution of the phases. But the coarsening also depends on the composition of the polymer blends. Only if the volume fraction of the minor phase is above the critical concentration at which the droplets of the minor phase actually touches, coarsening occurs in droplet-in-matrix via coalescence and in case of co-continuous morphology, the coalescence occurs by breakup only when the volume fraction of the minor phase is below a certain critical concentration and if the volume fraction of the minor phase is above a certain critical concentration, then breakup does not occur and the coalescence occurs only by retraction of the phases. (Willemse et al., 1999) Coarsening is an undesirable factor which is addressed by many researchers since coarsening tends to prevent the formation of co-continuous morphology and as stated obtaining a co-continuous morphology is one of the major goals in our project.

During annealing, the structure of the polymer blends relaxes with due course of time as a result of which the domain size of the constituents of the polymer blends increases. During the coarsening of the phases while annealing, the blend morphology is difficult to be controlled. (Liu et al., 2014) So, in order to maintain a co-continuous morphology throughout, the coarsening of the phases needs to be controlled. The coarsening of the phases can be controlled by introduction of fillers in the polymer blends which has a major influence on the morphology of the polymer blends.

The addition of fillers to immiscible polymer blends serves various purposes like enhancement of the mechanical properties and obtain high electrical conductivity. The fillers can also control the coarsening as mentioned above by serving as a barrier at the interface of the polymer phases in the polymer blends preventing the migration and mechanical mixing. In case of PS/PMMA

blends, increase in the content of fillers like carbon black increases the fineness of the blends suppressing the coarsening of the constituents of the polymer blends (Scherzer et al., 2015).

There are various factors that affect the morphology of the blends which can be stated as composition, processing methodologies and the interfacial tension. The effect of these aspects is briefly described in this report. Starting with the impact of the composition of the blends, composition has a very prime role in determining the morphology of the blend. From the literature, we know that there are various types of morphology like fibrillar, co-continuous, droplet-in-matrix morphology. The important morphologies which are of our concern are co-continuous and droplet-in-matrix morphology out of which the latter is the most stable morphology. But in view of obtaining a low percolation threshold maintaining a continuous conductive network, a co-continuous morphology is preferable. So, for obtaining a co-continuous morphology, composition of the system must be carefully maintained else we will obtain a phase separated blend as observed by N.Rozik et al (Rozik et al., 2016). The composition of the blend is not limited to the concentration of the polymers making up the blend but also the amount of fillers required to form a continuous conductive network.

The next factor which has a crucial role in determining the morphology is the processing method. By processing methods we mean the mixing sequence and introduction of compatibilized fillers in the blends. The effect of both of the above mentioned factors are discussed below.

The influence of mixing sequences has been well illustrated by B.Lin et al (Lin et al., 2006). They have observed that the order in which the polymers are mixed with the fillers are of prime importance as they determine the mobility of the fillers in the blends.

The rheological properties which play a major role in the field of polymer blends are viscosity, shear stress, shear rate, storage modulus and the loss modulus. One of the first relation to correlate the viscosity of a blend to the viscosity of its components is given by Equation 1.5:

$$\eta_b = \eta_1\phi_1 + \eta_2\phi_2 \quad (1.5)$$

Where η_b refers to the viscosity of the blend, η_1 , η_2 refer to the viscosity of the individual constituents and ϕ_1 , ϕ_2 refer to the volume fraction of the individual constituents in the polymer blends.

In PS/PMMA blends, the researchers have observed a negative deviation from the additivity rule of the viscosities suggesting a weak adhesion between the polymers of PS and PMMA at the interfaces. S.R. Vashishtha et al (Vashishtha et al., 2002) also observed that there is a change in the viscosity of the polymer blends when they are subjected to shear stresses and also with increase in the concentration of PMMA. H.K Chuang et al (Chuang & Han, 1984) in their research have pointed out the fact that in case of PS/PMMA blends, the trend of variation of the normal stress difference vs the shear stress and that of the storage modulus vs loss modulus is different for varying blend compositions irrespective of the temperature emphasizing the importance of the composition of the blends on the rheological properties. Several Emulsion models have been developed to correspond the linear viscoelastic response of the polymer blends to their morphology, composition and the interfacial tension between the components (Palierne's, Bousmina's models)

1.4. Conductive polymer blends

As reviewed above, the polymer blends have been gaining popularity in the field of conductive nanocomposites. The polymer blends can be made conductive by the addition of conductive nanofillers. But this issue is not that simple. All the factors which influence the formation of a conductive polymer blends needs to be carefully monitored. One of them being the morphology of the polymer blends. From the morphology point of view, one can also visualize that a co-continuous morphology aids in lowering the percolation threshold. After sorting out the issue of morphology, then the location of the conductive particles comes into play. The selective localization of the conductive nanoparticles at the interface helps in minimizing the percolation threshold but this also depends on a number of factors which are reviewed below:

- a) The concentration of nanoparticles added to the blends;
- b) The size of the nanoparticles introduced in the blend;
- c) The interfacial tension between the different components that will affect the wetting coefficient;
- d) The viscosity ratio of the polymers in the polymer blends;
- e) The mixing sequence of the polymers;
- f) A post-annealing of the conductive blend.

The effect of the most important of these factors are reviewed below:

- a) Wetting coefficient

The wetting coefficient can be formulated as in Equation 1.6 (Fenouillot et al., 2009):

$$\omega = \frac{\gamma_{A/GNPs} - \gamma_{B/GNPs}}{\gamma_{A/B}} \quad (1.6)$$

Where ω is the wetting coefficient and A and B are the polymers and GNPs are the graphene nanoplatelets, $\gamma_{A/B}$ denotes the interfacial tension between A and B There are certain conditions that need to be satisfied in order to selectively localize the graphene nanoplatelets to obtain a stable system which can be stated as in Table 1.5:

Table.1.5 Equilibrium condition for selective localization of graphene nanoplatelets
Adapted from Reza Salehiyan et al (Salehiyan & Ray, 2019)

Value of the wetting coefficient	Equilibrium condition for localization
$-1 < \omega < 1$	At the interface between A and B phases
$\omega < -1$	Stable in A phase
$\omega > 1$	Stable in B phase

The interfacial tension between the polymers and the fillers can be evaluated using Equation 1.7 .

$$\gamma_{A/B} = \gamma_A + \gamma_B - 2\sqrt{\gamma_A^d \gamma_B^d} - 2\sqrt{\gamma_A^p \gamma_B^p} \quad (1.7)$$

Where γ^d and γ^p are the dispersive and polar components of the surface energies at the processing temperatures.

According to the equilibrium condition, if the nanoparticles are placed in a more stable polymer phase, the graphene nanoplatelets will be agglomerated in that phase and which will in turn increase the viscosity of the polymer system and disrupt the stability of the whole polymer system. Therefore, it is better to start with the polymer phase which is less thermodynamically favorable so that the graphene nanoplatelets migrate towards the more stable phase and get trapped at the interface which is a more efficient location for obtaining a conductive material.

b) Viscosity ratio

As discussed above, the phase inversion from the droplet-in-matrix morphology to co-continuous morphology depends on the viscosity ratio. So, the maintenance of a definite morphology depends on the viscosity ratio which affects the selective localization of the nanoparticles in the polymer blends. The selective localization of the nanoplatelets is dependent on the wetting coefficient. The wettability of the nanoparticles depends on the viscosity ratio of the polymer phases in the blends.

L. Bai et al (Bai et al., 2018) observed that the selective localization of graphene nanoplatelets takes place according to theory of wetting coefficient as discussed previously. They considered PLA (Poly Lactic Acid) as A phase and PS (Polystyrene) as B phase. They evaluated the wetting coefficient for blends of PLA and PS which was found to be 2.73, and concluded that the graphene nanoplatelets should be thermodynamically get located in the PS phase according to the Equation 1.6

Therefore, during melt compounding, they suggested that the graphene nanoplatelets need to be mixed with the less favorable phase i.e. PLA phase, so that during annealing, the graphene nanoplatelets will get transported completely towards the more stable phase (PS) and get accumulated at the interface between the PS and PMMA phases. They also studied the effect of the mixing sequences and observed that if the following mixing sequence (PLA/GNPs)/PS was followed, then some of the graphene nanoplatelets will get trapped at the interfaces and only some will be observed in the PS phases but if (PS/GNPs)/PLA mixing sequence was followed, then all of the graphene nanoplatelets will be observed in the PS phase but in agglomerated condition tending to increase the viscosity of the system. One of the major aims of their project was to suppress the coarsening condition which was achieved by controlling the annealing time and annealing temperature. They have reported that when the content of the GNPs was increased from 0.5 weight% to 2 weight%, the characteristic domain size after getting stabilized was found to decrease considerably (from 16 μ m to 2.5 μ m) and the time required for achieving the maximum domain size in the presence of the graphene nanoplatelets. They found that the coarsening suppression could also be correlated to the compounding time. They observed that the suppression of coarsening was better when the polymers were compounded for 30 seconds than when compounded for 10 or 30 minutes. One of the challenges experienced was the non-uniform dispersion of graphene nanoplatelets which they tried to solve by the chemical modification of the graphene nanoplatelets. But, while improving the dispersion of the graphene nanoplatelets, they observed that the value of conductivity had been compromised.

R. Altobelli et al (Altobelli et al., 2017) also studied the tuning of the domain sizes with the help of the nanoparticles thereby suppressing the coarsening effect of the polymer phases. They

also emphasized on the selective localization of the nanoparticles in order to retain a thermodynamic stable system. E.Helal et al (E. Helal et al., 2019) focused on the correlation between the rheological behavior, electrical conductivity and the co-continuity of the morphology of the linear low density polyethylene/Ethyl Vinyl Acetate (LLDPE/EVA) blends filled with graphene nanoplatelets. Their study also focused on the evolution of the properties of the blends during thermal annealing and stabilization of the morphology of the blends during thermal annealing. Various scaling relations were developed to correlate the electrical and rheological percolation thresholds with the dispersion of the particles and change in the morphology of the blends.

c)Size of the nanoparticles added to the blends

The migration or the movement of the nanoparticles in the blends may occur via diffusion of the nanoparticles due to their Brownian motion and the diffusion strongly depends on the viscosity as already discussed above and also on the size of the nanoparticles introduced in the blends.

R. Salehiyan et al (Salehiyan & Ray, 2019) reviewed the basics of the migration of the conductive nanoparticles on the selective localization of the nanoparticles and the electrical properties of the blends. They also studied that the wetting coefficient mainly controls the selective localization of the nanoparticles. They also studied that various other factors like mixing sequence, intensity, viscosity ratio, mixing time, size and shape of the nanoparticles also influence the selective localization of the nanoparticles. Rate of migration of the nanoparticles also depends on the aspect ratio of the nanoparticles.

Migration of the nanoparticles occur via Brownian motion of the nanoparticles through the polymer phases. The rate of migration can be defined by the time required by a nanoparticle to travel a distance equal to its diameter which can be calculated using the equation 1.8

$$t_D = \frac{d^2}{4D_{ro}} \quad (1.8)$$

Where d= diameter of the nanoparticle; D_{ro} = Rotary Diffusivity of the nanoparticles.

Diffusion of the nanoparticles through the polymer phases can be defined by rotary diffusivity (D_{ro}) which is given by Equation 1.9 for platelet like particles.

$$D_{ro} = \frac{3k_B T}{4\eta_s d^3} \quad (1.9)$$

Where k_B = Boltzmann's Constant; T = temperature; η_s = viscosity; D = diameter of the disk

Hence, from Equation 1.8 and Equation 1.9, it can be suggested that the nanoparticles with higher aspect ratio will migrate faster in the polymer phases than the nanoparticles with lower aspect ratio

To summarize, one could suggest that all the factors mentioned above were crucial in manipulating the blend morphology and increasing the stability of the morphology. The effect of filler content on the morphology was negligible beyond the critical filler content but once the filler content surpasses the critical filler content, the stress bearing ability of the polymer system tend to get decreased because of the agglomeration of the fillers.

In the current literature, very few works have emphasized the evolution of morphology of the blends and the correlation between the morphology, electrical and rheological behavior of the blends filled with the graphene nanoplatelets but no work has been conducted to study the effect of the size of conductive nanoparticles on the electrical and rheological behavior of the co-continuous blends and also study of the effect of the size of the graphene nanoplatelets on the evolution of the morphology and change in electrical and rheological properties during thermal annealing.

CHAPTER 2

OBJECTIVES

In view of the points stated above, we can now clearly state the objectives of this project. The primary objective of the project can be stated as follows:

Evaluation of the effect of the size of the graphene nanoplatelets on the design of graphene filled binary blend nanocomposites

The secondary objectives of the project are as follows:

- Determine the size effect of the graphene nanoplatelets on the kinetics of the migration of the graphene nanoplatelets towards the interface.
- Understand the size effect of graphene nanoplatelets on the rheological properties of the graphene filled polymer nanocomposites.
- Understand the size effect of graphene nanoplatelets on the electrical properties of the graphene filled polymer nanocomposites

In order to fulfill the objectives, the following research strategy was followed:

- a) Selection of a model immiscible polymer blend whose morphology is known
- b) Determination of the composition ratio of the polymers to obtain a co-continuous morphology
- c) Analyzing the various parameters like percolation threshold in order to determine the best suitable morphology of the polymer blend to obtain a conductive composite
- d) Determination of the mixing sequence of the polymers with the fillers
- e) Selective localization of the fillers in the polymer blends
- f) Characterization of the polymer blends (rheological, conductivity, surface morphology)
- g) Studying the effect of lateral size, surface area, by varying the grades of graphene
- h) Studying the effect of annealing time, temperature on the morphology and the properties of the polymer blends

CHAPTER 3

EXPERIMENTAL

3.1. Choice of materials

3.1.1. PS

Polystyrene (PS from INEOS Styrenics, Grade Empera 350N) was chosen in this work as one of the polymers for fabrication of the polymer blend. (Materials, 2001) The properties of the polystyrene can be stated as follows in 3.1.

Table 3.1 Properties of Polystyrene (PS)
Adapted from INEOS Styrenics (Styrenics)

Typical properties	Value
Density	1.19 g/cc
Melting temperature range	200-250°C
Grade	EMPERA 350N
Melt Volume Rate	1.5 (200°C/5 g)
Zero Shear Rate Viscosity at 200°C	9800 Pa.s
Viscosity at 170°C	429000 Pa.s

3.1.2. PMMA

PMMA was chosen as the other polymer for the fabrication of the polymer blends. In this project, we shall be using PLEXIGLASS 6N as the grade of PMMA. Some of the properties of PMMA can be stated in Table 3.2.

Table 3.2 Properties of Polymethylmethacrylate (PMMA)
Adapted from PLEXIGLAS Polymers (PLEXIGLAS)

Typical properties	Value
Density	1.18
Melting temperature range	220-240°C
Grade	PLEXIGLASS 6N (Evonik)
Melt Volume Rate	12 (230°C/3.8 kg)
Zero shear rate viscosity at 200 °C	12000 Pa.s

3.1.3. Graphene nanoplatelets

3.1.3.1. Characteristics of graphene nanoplatelets

The graphene nanoplatelets which are used in this project have varying properties and they can be graded as Grade C and Grade H. Both of the graphene nanoplatelets used have different lateral sizes, different surface areas and the effect of these properties of the graphene nanoplatelets are studied on the morphology and properties of the polymer blends. The specifications of the grades of the graphene nanoplatelets are mentioned in Table 3.3.

Table 3.3 Specifications of different grades of graphene used in this project

Grade of Graphene	Thickness (nm)	Particle size (um)	Surface area (m ² /g)
Grade C (ALDRICH)	Few nm	<2	750
Grade H (ALDRICH)	15	25	50-80

3.2. Methodology

3.2.1. Processing Methods

Melt mixing by extrusion (HAAKE PolyLab 900) was used to prepare the masterbatches with a profile temperature of 220°C in all zones with a screw speed of 80 rpm and feeding rate was kept at 5%. The composites were then prepared from the masterbatches by varying the concentration of the graphene nanoplatelets using twin screw extruder (HAAKE Minilab II) and the temperature was set at 200°C. PS/PMMA/GNPs blends were prepared by either premixing PMMA with GNPs (PMMA masterbatch or PMMA MB) or PS with GNPs (PS masterbatch or PS MB). The masterbatches were then mixed with either PS (PMMA MB) or PMMA (PS MB) to produce blends having different graphene concentration.

Samples for the rheological and conductivity measurements were prepared by compression molding at 200°C and the conditions at which the samples were pressed varied for samples filled with different grades of graphene.

The conditions of pressing are as follows:

Samples filled with grade C: pressed for 5 minutes at a pressure of 0.8 MPa followed by 5 minutes at a pressure of 5 MPa.

Samples filled with grade H: kept for 10 minutes at 200°C without applying any pressure followed by 5 minutes of pressing at 0.8 MPa and then pressed for 5 minutes at a pressure of 5 MPa. This was done to remove the roughness and homogenize the surface of the samples filled with grade H.

3.2.2. Rheological Properties

A capillary rheometer (SR 2, Instron) was used to measure the viscosity of the polymers at 200°C as a function of shear rates (1 s^{-1} to 1000 s^{-1}). The other rheological measurements were carried out with a rotational rheometer (MCR 501, Anton Paar) to evaluate the evolution of microstructure of the composites and the blends in their molten state at 200°C using a 25 mm parallel plate configuration and a sample gap of 0.9 mm. The dynamic strain sweep tests were performed to determine the linear viscoelastic region. The strain amplitude was varied from

0.01 to 10% and the tests were repeated for 3 different frequencies: 1, 10 and 100 rad/s to determine the linear viscoelastic region. Small Amplitude Oscillatory Shear tests were carried out in the linear viscoelastic region under selected strains from 0.25 to 0.46 %, which corresponded to the LVE. The angular frequency was varied from 300 rad/s to 0.01 rad/s.

3.2.3. Electrical Properties

Dielectric spectroscopy is used for characterizing the dielectric properties of a polymer blend as a function of frequency. It is manipulated on the basis of the interaction of the external electric field with the intrinsic dipole moment of the sample. Complex Permittivity was measured from 0.01 Hz to 300 kHz by applying 3 V_{rms} across the sample (corresponding to approximately 7.5 V/mm). The complex conductivity can be related to the complex permittivity ($\epsilon^*(\omega)$) which can be expressed in terms of the real ($\epsilon'(\omega)$) and imaginary parts ($\epsilon''(\omega)$) which can be noted in Equation 3.1:

$$\epsilon^*(\omega) = \epsilon'(\omega) - i\epsilon''(\omega) \quad (3.1)$$

The complex conductivity can be expressed in terms of frequency ($\sigma^*(\omega)$) in terms of real and imaginary parts by Equation 3.2:

$$\sigma^*(\omega) = \sigma'(\omega) + i\sigma''(\omega) \quad (3.2)$$

And thus, the complex conductivity can be related to the dielectric permittivity by the Equation 3.3:

$$\sigma^* = i\omega\epsilon_0\epsilon^* \quad (3.3)$$

Where ϵ_0 represents the vacuum permittivity, ϵ^* refers to the complex permittivity, ω refers to the angular frequency and σ^* refers to the complex conductivity. The conductivity values presented in this work refer to the conductivity values at the lowest values of the frequency (in this case 0.01 Hz) since at low frequencies, the real part of conductivity (σ') tends to have a direct current behavior. Discs of 25 mm diameter and around 1.2 mm in thickness were used. All samples were coated on both sides with 7.5 nm of gold (K550 X sputter coater, Quorum Technologies) to remove the effect of contact resistance.

3.2.4. Morphology Characterization

Scanning electron microscopy (SEM) was performed to observe the surface of samples. A S3600N microscope (Hitachi) at 5kV in secondary electrons mode was used. The samples were coated with gold (K550 X sputter coater, Quorum Technologies). ImageJ was employed to treat the images and calculate the characteristic domain size ξ , defined as the total area per total interfacial length. Three images of each composition were used to calculate the average ξ value.

CHAPTER 4

RESULTS AND DISCUSSIONS

4.1. Analysis of wetting coefficient theory for PS/PMMA blends

Table 4.1 presents the surface tension values (γ) and their respective polar (γ^p) and dispersive components (γ^d) for all the three components in the polymer blends which were used to evaluate the chemical affinity in the PS/PMMA/GNP system. The surface tension of the GNPs is higher than both the polymers (both γ^p and γ^d) while the total surface tension of PS is comparable to that of PMMA. Equation 1.7 was used to calculate the interfacial tension $\gamma_{A/B}$ between each pair of components: $\gamma_{A/B}=2.8 \text{ mN m}^{-1}$ for PS/PMMA, $\gamma_{A/B}=4.3 \text{ mN m}^{-1}$ for PMMA/GNPs, $\gamma_{A/B}=7.54 \text{ mN m}^{-1}$ for PS/GNPs. These values were used to determine the wetting coefficient which could estimate the equilibrium morphology of the system. The results suggest that in the equilibrium state GNPs have more affinity towards the PMMA phase and tends to be embedded in this polymer. The GNP filled PMMA phase is then mixed with PS phase. But owing to the similarities in the surface tension of PS and PMMA, the preference of GNPs filled PMMA phase in PS is weak. Therefore, the equilibrium is close to the boundary of PMMA phase and the interface between the PS and PMMA phases according to the wetting coefficient.

On the basis of the possible equilibrium state, in case of filled single polymer phases, GNPs have more affinity towards PMMA phase and get accumulated in PMMA phase rather than in PS phase. In case of blends, if a PS/GNP masterbatch is used, the inclusion of PMMA phase will trigger the migration of the GNPs towards the PMMA phase from PS phase when enough time is given for the migration. By using a PMMA/GNP masterbatch, no migration is expected theoretically. This can be clarified by the morphological characterization.

Table 4. 1 Surface tensions of the materials

Material	γ	γ^d	γ^p
PS	27.8	21.9	3.9 (Elias et al., 2007)
PMMA	27.4	19.6	7.7 (Taguet et al., 2014)
GNPs	53	39.1	13.9 (Kozbial et al., 2014)

But, the migration of the GNPs not only depend on the wetting coefficient but also on their respective surface areas and lateral sizes and the analysis of the lateral sizes of GNPs on the migration in a certain phase is discussed in the next section.

4.2. Analysis of the diffusion of GNPs in the polymer system

The migration of plate-like particles in a polymer system can be determined by equation 1.9 which depicts the rotary diffusivity of rigid disks (D_{r0}) (Filippone et al., 2014). Considering the values of viscosity at a shear rate of 100s^{-1} , the viscosity of PMMAMB is almost the double of that of PSMB according to Figure 4.4 (3347.81 Pa.s vs. 1367.75 Pa.s) for filler having higher surface area (Grade C) and the viscosity of PMMAMB is almost the double of that of PSMB according to Figure 4.4 (2786.19 Pa.s vs. 1060.50 Pa.s) for filler having lower surface area (Grade H) as well. Consequently, the diffusivity of GN particles (both Grade C and Grade H) in PSMB is expected to be 2 times higher or larger particles are expected to diffuse. The time scale for the rearrangements of the GNP networks can be roughly correlated with the inverse of the rotary diffusivity (Filippone et al., 2014). Particles with larger lateral dimensions will require higher temperature/lower viscosity to be able to diffuse.. Table 4.2 presents the rotary diffusivity of GNP grade C and grade H in both PS and PMMA.

Table 4.2 Rotary Diffusivity and the rate of migration of the different grades of GNPs in the polymers

Filler	Size (μm)	Rotary Diffusivity		Rate of migration	
		In PS	In PMMA	In PS	In PMMA
GNP Grade C	<2	4.5E-7	1.82E-7	2.2E-6	5.49E-6
GNP Grade H	25	2.954E-10	1.124E-10	0.53	1.39

From the table 4.2, it can be observed that the particles with smaller dimensions (Grade C) diffuse faster than the particles with larger dimension (Grade H) and they migrate at a faster rate in the polymer phases. The particles with larger dimension require lower viscosity polymer phase to migrate or diffuse through

4.3. Influence of adding graphene nanoplatelets on the pure phases

4.3.1. Results

Figure 4.1 presents the electrical conductivity as a function of concentration of graphene for both grades of graphene filled in pure phases PS and PMMA. Introduction of graphene nanoplatelets increases the electrical conductivity of filled polymer phases irrespective of the polymer phases. It can be seen that in case of filled PS phase, with increase in concentration of the graphene grade H, there is an increase in the value of electrical conductivity up to a value of 0.01 S/m whereas in case of graphene grade C, there is no such significant increase in the value of conductivity. In case of filled PMMA phase, it can be observed that with increase in concentration of both the grades of graphene nanoplatelets, there is significant increase in the value of conductivity up to 0.1 S/m (in case of graphene grade H) and 0.001 S/m (in case of graphene grade C).

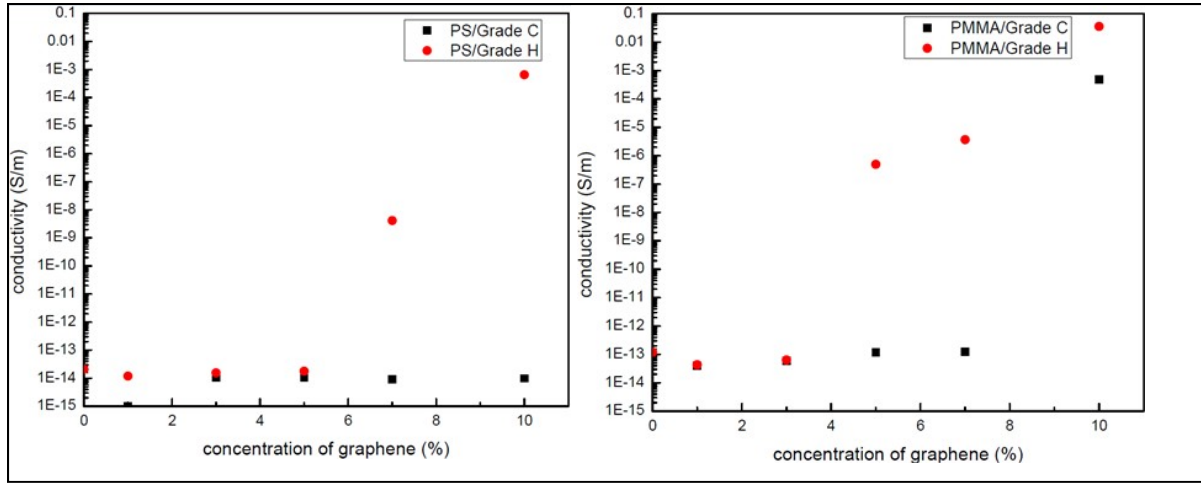


Figure 4.1 Electrical Conductivity as a function of concentration of GNPs for a)filled PS phases b)filled PMMA phases

Figure 4.2 presents the variation of storage modulus as a function of angular frequency for varying concentrations of graphene grade C and graphene grade H filled in pure phase PS. It can be seen that by adding graphene nanoplatelets in the pure phases, there is an increase in the storage modulus at all the observed frequencies. With increase in concentration of the graphene nanoplatelets irrespective of the graphene grade, the storage modulus increases and it also can be observed that the trend of increase in storage modulus is similar at higher frequencies for every sample tested. In case of pure phase PS filled with graphene grade H, there is no significant increase in the value of storage modulus up to a concentration of 7 wt% of graphene nanoplatelets as compared to the value of storage modulus of pure PS phase at lower frequencies whereas in case of pure PS filled with graphene grade C, there is an increase in the value of storage modulus even at a concentration of 5 wt% of graphene nanoplatelets as compared to the value of storage modulus of pure PS phase at lower frequencies. Table 4.3 presents the slopes of $\log G'$ vs $\log \omega$ of filled PS phases with graphene Grade C and Graphene Grade H where G' represents storage modulus and ω represents the angular frequency at lower frequencies from 0.01 – 0.08 rad/s

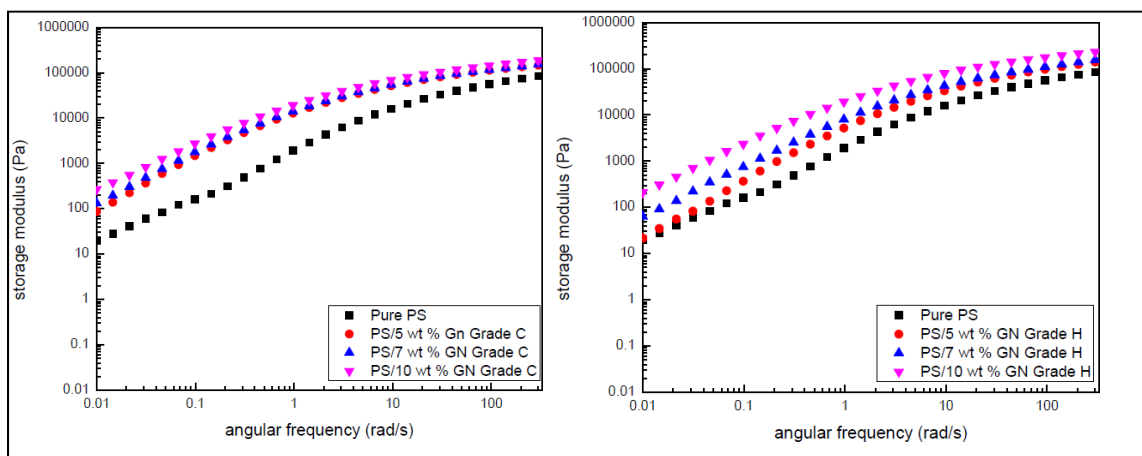


Figure 4.2: Storage modulus as a function of angular frequency for a)PS filled with grade C b)PS filled with grade H

Table 4.3 Slope analysis of $\log G'$ vs $\log \omega$ at lower frequencies (0.01-0.08 rad/s) for filled PS phases

PS			
Concentration of Graphene Grade C	Slope of $\log G'$ vs $\log \omega$ at lower frequencies	Concentration of Graphene Grade H	Slope of $\log G'$ vs $\log \omega$ at lower frequencies
0	2	0	2
5	1.24	5	1.23
7	1.14	7	1.10
10	1.02	10	1.07

Figure 4.3 presents the variation of storage modulus as a function of angular frequency for varying concentrations of graphene grade C and graphene grade H filled in pure phase PMMA. It can be seen that by adding graphene nanoplatelets in the pure phases, there is an increase in the storage modulus at all the observed frequencies. With increase in concentration of the graphene nanoplatelets irrespective of the graphene grade, the storage modulus increases and the trend of increase in storage modulus is similar at higher frequencies for every sample tested. In case of pure phase PMMA filled with graphene grade C, it can be observed that there is a plateau present at lower frequencies and in case of pure phase PMMA filled with graphene

grade H, it can be observed that the storage modulus increases with increase in concentration but there is no plateau observed. Table 4.4 presents the slope analysis of $\log G'$ vs $\log \omega$ of filled PMMA phases with graphene Grade C and Graphene Grade H where G' represents storage modulus and ω represents the angular frequency at lower frequencies from 0.01 rad/s to 0.08 rad/s

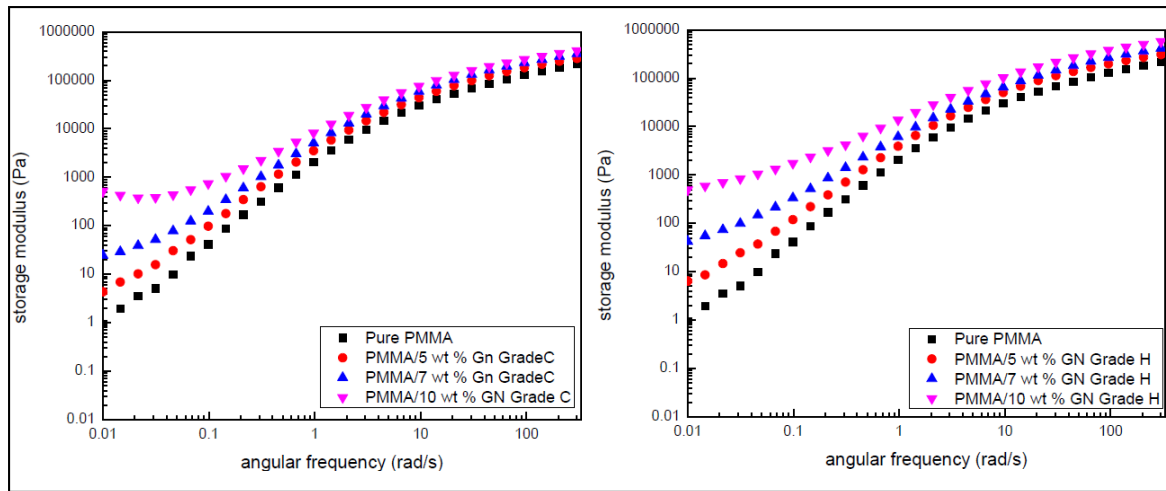


Figure 4.3 Storage modulus as a function of angular frequency for a) PMMA filled with grade C b) PMMA filled with grade H

Table 4.4 Slope analysis of $\log G'$ vs $\log \omega$ at lower frequencies (0.01 -0.08 rad/s) for filled PMMA phases

PMMA			
Concentration of Graphene Grade C	Slope of $\log G'$ vs $\log \omega$ at lower frequencies	Concentration of Graphene Grade H	Slope of $\log G'$ vs $\log \omega$ at lower Frequencies
0	1.62	0	1.62
5	1.35	5	1.29
7	0.92	7	0.90
10	0.17	10	0.54

Thus, from above observations, it can be suggested that there are various parameters like the polymer phases, size of graphene nanoplatelets and concentration of graphene nanoplatelets

which have significant effects on the characterization of the properties of the pure phases filled with graphene nanoplatelets. The influence of all these parameters are discussed below.

4.3.2. Discussions

4.3.2.1. Concentration of the graphene nanoplatelets

From figure 4.1, one can easily observe that there is a significant increase in the values of conductivity with the increase in concentration for all the materials tested in this project but the trend of increase in the values of conductivity varies for each material. This can be explained by the onset of the electrical percolation network in the samples tested. From Figure 4.1, it can be suggested that the GN percolation starts at concentrations varying between 4 to 8 wt% of graphene nanoplatelets and is different for different materials and the highest conductivity values for different samples can range from 0.001 S/m to 0.1 S/m. This trend can be verified by the rheological characterization of the samples.

Rheological characterization is performed to investigate the formation of a solid rigid network of the graphene nanoplatelets in the pure polymer phases. From figure 4.2, it can be observed that there is an increase in the storage modulus with increase in concentrations of graphene nanoplatelets and there is a similarity in the trend of the storage modulus at higher frequencies and as observed in the characterization of electrical properties, the trend is different for different materials. This can be further explained by the variation in the onset of the formation of the rigid network in the samples tested which can be estimated by observing the trend of slope of the storage modulus at lower angular frequencies. The analysis of the slope gives an idea about the formation of the rigid network which restricts the deformation of the polymer phases.

As can be seen from Table 4.3 and Table 4.4, the slope of the storage modulus of the filled polymer phases is lower than the slope of the storage modulus of pure polymer phases and the slope decreases with increase in the concentration of the graphene nanoplatelets indicating the addition of the graphene nanoplatelets act to decrease the movement of the polymer chains but the trend is different for different materials tested and is dependent on the polymer matrix and

size of the graphene nanoplatelets. The influence of these parameters is discussed in the following subsequent sections

4.3.2.2. Polymer Matrix

As discussed, the characterization of the electrical and rheological properties is significantly influenced by the concentration of the graphene nanoplatelets. They are also influenced by the variation of polymer matrix. From Figure 4.1, it can be observed that there is a remarkable difference in the trend of electrical conductivity with variation in polymer matrix. In both filled polymer phases, one of the similarities that can be observed is that there is an increase in electrical conductivity with increase in concentration of the graphene nanoplatelets but the most remarkable difference between both the filled polymer phases is the onset of percolation threshold in the filled polymer phases. In case of filled PS phase, the percolation of the graphene nanoplatelets starts at a concentration between 5 and 7 wt% of graphene nanoplatelets and in case of filled PMMA phase, the percolation of the graphene nanoplatelets starts at a slightly lower concentration between 3 and 5 wt% of graphene nanoplatelets. However, there is a difference in trend of the electrical properties also with the variation of grade of graphene nanoplatelets which will be discussed in the next section. The difference in the properties will be further confirmed by the characterization of the rheological properties.

Rheological properties are characterized by observing the variation of the storage modulus with angular frequencies. The slope of storage modulus vs frequency at low frequencies gives an estimate of the solid state of the network formed in the samples. From Figure 4.2, it can be very well observed that there is an increase in the storage modulus with increase in concentration of the graphene nanoplatelets in both the filled polymer phases and the trend of the increase in storage modulus is similar for all the samples at higher frequencies but the trend of increase in storage modulus at lower frequencies is significantly different for the filled PS phases and filled PMMA phases. From Figure 4.3, it can be observed that there is a plateau formed at lower frequencies for filled PMMA phases at a concentration of 10 wt% of graphene nanoplatelets whereas from Figure 4.2, it is observed that there is no plateau formed at lower frequencies for filled PS phases even at 10 wt% of graphene nanoplatelets. This suggests that in PMMA, the graphene nanoplatelets have successfully formed a rigid network in the sample

restricting the mobility of the PMMA chains at higher concentrations of the graphene nanoplatelets which is not the case of filled PS phases. This can be further confirmed by observing the slope analysis of the filled phases at lower concentration. From Table 4.3 and Table 4.4, it can be observed that there is a significant difference in the slopes at lower frequencies for filled PS and PMMA phases. In case of filled PMMA phases, with increase in concentration of the graphene nanoplatelets, the slope decreases with respect to the slope of pure phases indicating that the graphene nanoplatelets act as fillers and form a solid network in PMMA phase whereas in case of filled PS phases, there is a decrease in the slope with increase in concentration but the decrease in slope is less and the values of the slopes at lower frequencies of the filled PS phases is higher than the slope of pure PS phase indicating the poor dispersion of the graphene nanoplatelets in PS phase. However, there are differences in each of the filled phases with variation in size of graphene nanoplatelets which is discussed in the next section.

4.3.2.3. Size of the graphene nanoplatelets

From Figure 4.1, 4.2 and 4.3, it can be clearly observed that irrespective of the polymer matrix, there is a significant difference in the characterization of the electrical and rheological properties of the polymer phases filled with different sizes of graphene nanoplatelets. From Figure 4.1, there is a remarkable difference in the values of electrical conductivities of the samples filled with Grade C and Grade H. In case of PS, as observed from Figure 4.1 a), the GN percolation starts at a concentration between 5 and 7 wt% of graphene nanoplatelets for PS phase filled with Graphene Grade H and the highest conductivity value is in the range of 0.001 S/m at a concentration of 10 wt% of graphene nanoplatelets whereas there is no apparent increase in the value of conductivity for PS phase filled with Graphene Grade C till a concentration of 10 wt% of graphene nanoplatelets with the value of highest conductivity in the range of 10^{-14} S/m. In case of PMMA, as observed from Figure 4.1 b), the GN percolation starts at a concentration between 3 and 5 wt% of graphene nanoplatelets for PMMA phase filled with Graphene Grade H and the highest conductivity value is in the range of 0.1 S/m whereas the GN percolation starts at a concentration between 7 and 10 wt% of graphene nanoplatelets for PMMA phase filled with Graphene Grade C and the highest conductivity

value is in the range of 0.01 S/m. Hence, it is clear that the size of graphene nanoplatelets has a significant influence on the characterization of electrical properties. This observation is further verified by the characterization of the rheological properties.

Rheological properties give an estimate of the deformation and flow behavior of the materials. From Figure 4.2 and 4.3, it can be clearly observed that the storage modulus increases with increase in the concentration of the graphene nanoplatelets but the trend of increase of storage modulus at lower frequencies is different for different size of graphene nanoplatelets filled in the polymer phases. In case of PMMA, as observed from Figure 4.2, there is a plateau formed at a concentration of 10 wt% of graphene nanoplatelets for PMMA phases filled with Graphene Grade C whereas in case of PMMA phases filled with Graphene Grade H, the formation of plateau seems to be on the verge of onset and it can be assumed that the plateau can be seen to be fully developed at a concentration slightly higher than 10 wt% of graphene nanoplatelets. In case of PS, as observed from Figure 4.3, neither the plateau nor the onset of the plateau formation can be observed in the PS phases filled with either Graphene Grade C or Graphene Grade H. These observations can be further analyzed by the slope analysis at lower frequencies.

From Table 4.3, it can be observed that in case of PMMA filled with Graphene Grade C, the slope of storage modulus versus angular frequency decreases with respect to the slope of pure phases but in case of PMMA filled with Graphene Grade H, the decrease in slope is more predominant thereby suggesting a good dispersion of graphene nanoplatelets in the PMMA phase but at a concentration of 10 wt% of graphene nanoplatelets, PMMA phases filled with Graphene Grade C has a slope lower than that filled with Graphene Grade H. This indicates that a higher concentration of graphene Grade C, these GNPs are more uniformly dispersed and a solid like network is formed which decreases the mobility of the PMMA phases whereas in case of Graphene Grade H, the dispersion is improved significantly at lower concentration of GNPs but then gradually increases. So, in case of Graphene Grade H, there is an onset observed for the formation of the solid like network which is not totally developed till a concentration of 10 wt% of GNPs. In case of filled PS phases, as observed from Table 4.4, both the grades of graphene nanoplatelets are poorly dispersed as a result of which there is no plateau formed in any of the filled PS phases

Thus, it can be concluded that the percolation threshold is relatively high in case of filled pure phases. So, in order to optimize the cost of the materials, the percolation threshold should also be optimized for which we will be fabricating co-continuous morphology as explained in the research strategy. Therefore, blends will be fabricated in order to have a co-continuous morphology to reduce the percolation threshold and the composition of the blends is deduced by analyzing the trend of viscosity vs shear rate and using the constitutive equation of rheology ($\eta_1/\eta_2 = \phi_1/\phi_2$) where η represents the viscosity and ϕ represents the volume fraction of the polymer phases. The design of the blends and how the use of blends affect the electrical and rheological percolation threshold of the material will be presented in the next section.

4.4. Use of blend to decrease the percolation threshold of the material

4.4.1. Choice of concentration for polymer blend

As shown in the literature review, in order to get a co-continuous morphology one should choose a volumic concentration of both polymer so that it fits by Equation 1.4

Figure 4.4 presents the viscosity as a function of shear rate for pure PMMA, pure PS, filled PMMA phases and filled PS phases. It can be observed that the trend of increase of viscosity with shear rate is similar for all the samples tested. It can be observed that the viscosity values for PMMA at any shear rate value is double that for PS. This can be used to deduce the composition ratio of PS/PMMA in the blend in order to have a co-continuous morphology using Equation 1 using the viscosities of PS and PMMA respectively at a shear rate of 80 1/s, the volume fraction of PS/PMMA comes out to be 30/70. Thus, the composition ratio of PS/PMMA in the blends to obtain a co-continuous morphology should be in the ratio of 30/70.

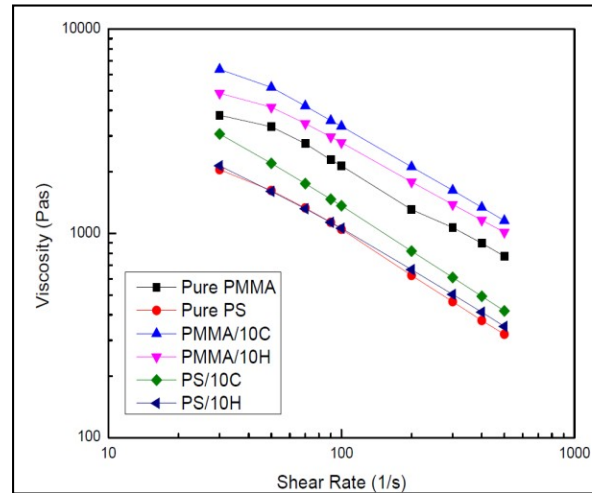


Figure 4.4 Viscosity vs shear rate for pure polymer phases (PS & PMMA) and filled polymer phases (PS and PMMA)

Figure 4.5 and 4.6 present the micrographs of the neat blends of PS and PMMA with PS/PMMA in the ratio of 30/70 and 50/50. From the figures, it can be suggested that the blend with PS/PMMA in the ratio of 30/70 presents more of a droplet in matrix morphology whereas the blend with PS/PMMA in the ratio of 50/50 presents a co-continuous morphology instead. Thus, it can be suggested that the blend with PS/PMMA in the ratio of 50/50 would be a preferable choice of blend as it presents more of a co-continuous morphology as explained in the research strategy

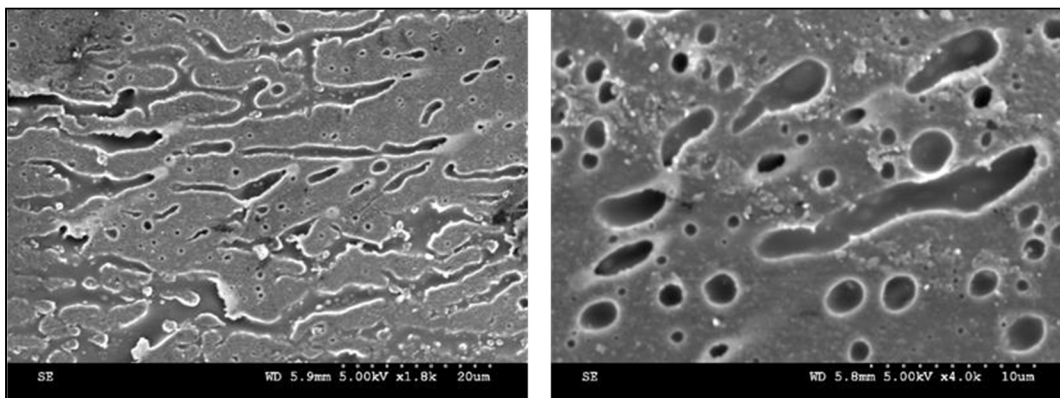


Figure 4.5 Micrographs of neat blends (PS/PMMA) in the ratio of (30/70)

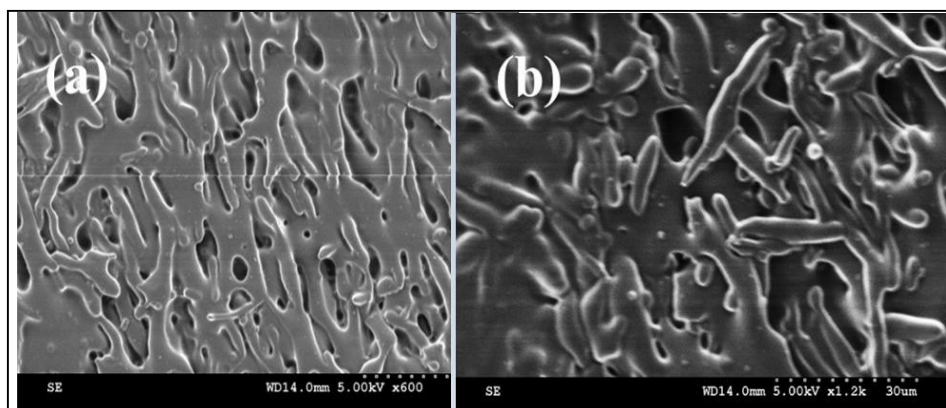


Figure 4.6 Micrographs of neat blends (PS/PMMA) in the ratio of (50/50)

Therefore, from now on in this work, the blends mentioned have PS and PMMA in the ratio of 50/50.

Effect of addition of graphene to the blends

4.4.1.1. Results

Figure 4.7 presents the conductivity value as a function of graphene concentration for PS/PMMA/GNPs blends filled with graphene nanoplatelets of both grades (Grade C and Grade H) formed from both of the masterbatches (PS Masterbatch (Figure 4.7 a) and PMMA Masterbatch (Figure 4.7 b)). Introduction of graphene in the PS/PMMA/GNP blends increases the value of conductivity but there is a significant difference in the trend of increase in the values of conductivity for each blend fabricated from varying masterbatches and also filled with varying graphene grades. In case of PS/PMMA/GNPs blends fabricated from PMMA masterbatch, the blends filled with Graphene Grade C has a significant increase in the value of conductivity up to the range of 10^{-1} S/m whereas on the other hand, in the case of blends filled with graphene grade H for the same increase in the concentration of graphene nanoplatelets, the increase in the value of conductivity is not significant and is in the range of 10^{-13} S/m up to 5 wt% of graphene nanoplatelets but when the concentration of the graphene nanoplatelets is increased up to 9 wt%, there is a significant increase in the value of conductivity up to the range of 10^{-5} S/m. Whereas in case of PS/PMMA/GNPs blends fabricated from PS

masterbatch, there is a significant increase in the value of electrical conductivity and lies around the range of 10^{-4} S/m irrespective of the type of fillers when the concentration of the graphene nanoplatelets is increased from 5 wt% up to 9 wt% of graphene nanoplatelets

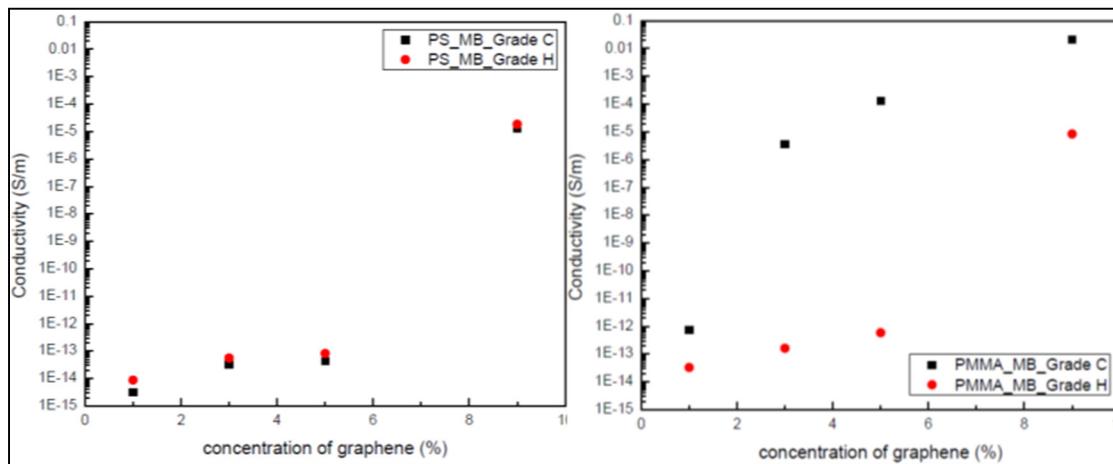


Figure 4.7 Electrical Conductivity as a function of concentration of GNPs for a)PS based blends b)PMMA based blends where PS/PMMA is in the ratio of 50/50

Figure 4.8 presents the variation of storage modulus as a function of angular frequency for varying concentrations of graphene grade C and grade H filled in PS/PMMA/GNPs blends fabricated from PS masterbatch. It can be observed that by adding graphene nanoplatelets in the pure blends, the storage modulus increases with increase in concentration at all the observed frequencies. It can also be observed that the trend of increase in storage modulus with increase in angular frequencies is similar at higher frequencies for all the samples tested irrespective of the type of fillers. In case of PS/PMMA/GNPs blends fabricated from PS masterbatch filled with graphene grade H, there is no significant increase in the storage modulus up to a concentration of 5 wt% of graphene nanoplatelets as compared to the storage modulus of pure PS/PMMA blend at lower frequencies but when the concentration of the graphene nanoplatelets is increased from 5 to 9 wt%, a plateau is observed at lower frequencies whereas in case of PS/PMMA/GNPs blends fabricated from PS masterbatch filled with graphene grade C, there is a significant increase in the storage modulus beyond a concentration of 3 wt% of graphene nanoplatelets when compared to the storage modulus of neat PS/PMMA

blend at lower frequencies but when the concentration of the graphene nanoplatelets is increased from 5 to 9 wt%, a plateau is observed at lower frequencies

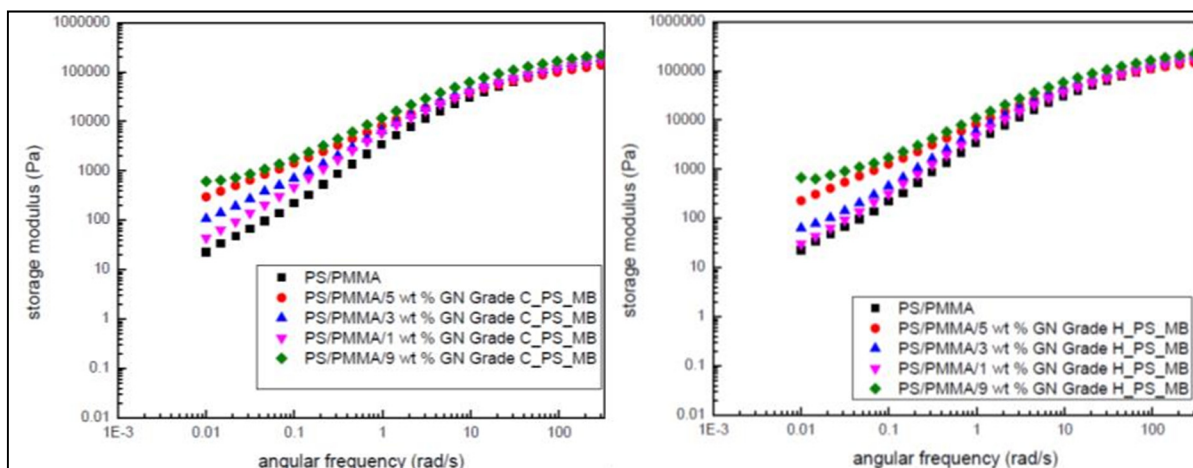


Figure 4.8 Storage Modulus as a function of angular frequency for PS based blends filled with Graphene a)Grade C and b)Grade H

Further analysis may be carried out by performing slope analysis of $\log G'$ vs $\log \omega$ at lower frequencies where G' represents the storage modulus and ω represents the angular frequency. Table 4.5 presents the slope analysis at lower frequencies (0.01 to 0.08 rad/s)

Table 4.5 Slope of $\log G'$ vs $\log \omega$ at lower frequencies (0.01 to 0.08 rad/s) for PS based blends filled with Graphene Grade C and Grade H

PS/PMMA/GNP blends_PS_MB			
Concentration of Graphene Grade C	Slope of $\log G'$ vs $\log \omega$ at lower frequencies	Concentration of Graphene Grade H	Slope of $\log G'$ vs $\log \omega$ at lower frequencies
0	0.95	0	0.94
1	0.84	1	0.89
3	0.77	3	0.85
5	0.63	5	0.66
9	0.52	9	0.45

Figure 4.9 presents the variation of storage modulus as a function of angular frequency for varying concentrations of graphene grade C and grade H filled in PS/PMMA/GNPs blends fabricated from PMMA masterbatch. It can be observed that by adding graphene nanoplatelets in the pure blends, the storage modulus increases with increase in concentration at all the observed frequencies. It can also be observed that the trend of increase in storage modulus with increase in angular frequencies is similar at higher frequencies for all the samples tested irrespective of the type of fillers but varies at lower frequencies. In case of PS/PMMA/GNPs blends fabricated from PMMA masterbatch filled with graphene grade H, it can be observed that there is an onset of the formation of plateau at a concentration of 3 wt% of graphene nanoplatelets whereas in case of PS/PMMA/GNPs blends fabricated from PMMA masterbatch filled with graphene grade C, there is a plateau observed at a concentration of even 1 wt% of graphene nanoplatelets.

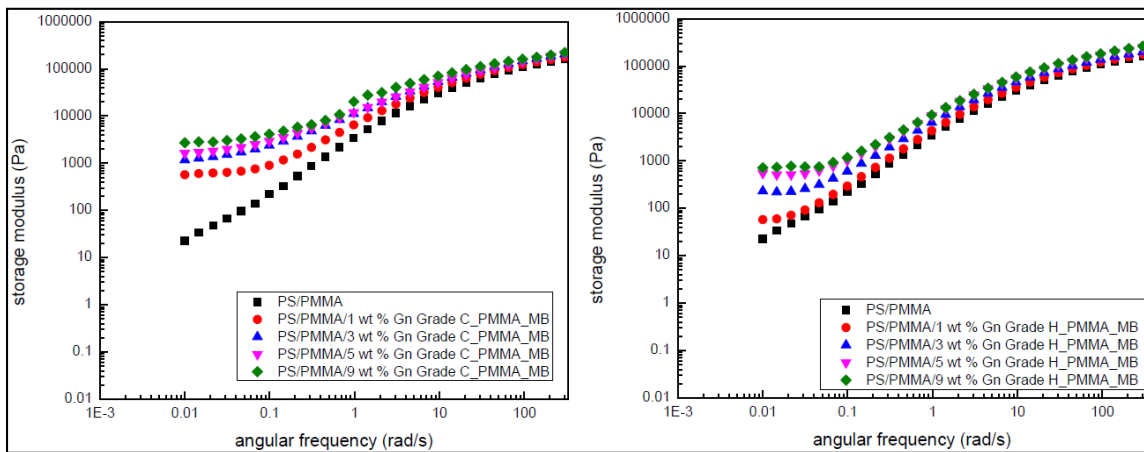


Figure 4.9 Storage Modulus as a function of angular frequency for PMMA based blends filled with Graphene a)Grade C and b)Grade H

Further analysis may be carried out by performing slope analysis of $\log G'$ vs $\log \omega$ at lower frequencies where G' represents the storage modulus and ω represents the angular frequency. Table 4.6 presents the slope analysis at lower frequencies (0.01 to 0.08 rad/s).

Table 4.6 Slope of $\log G'$ vs $\log \omega$ at lower frequencies (0.01 to 0.08 rad/s) for PMMA based blends filled with Graphene Grade C and Grade H

PS/PMMA/GNP blends _PMMA_MB			
Concentration of Graphene Grade C	Slope of $\log G'$ vs $\log \omega$ at lower frequencies	Concentration of ne Grade H	Slope of $\log G'$ vs $\log \omega$ at lower frequencies
0	0.92	0	0.92
1	0.66	1	0.88
3	0.57	3	0.77
5	0.54	5	0.71
9	0.18	9	0.18

Figure 4.10 presents the blend morphology of pure PS/PMMA blend (Figure 4.10 a) and PS/PMMA/GN blends fabricated from PMMA masterbatch (Figure 4.10 b (blends filled with graphene grade C) and Figure 4.10 c (blends filled with graphene grade H) after being extruded and subjected to compression molding. The neat blend presents a co-continuous morphology. There is a significant difference in the blends fabricated from PMMA masterbatch filled with graphene grade C and those fabricated from PMMA masterbatch filled with graphene grade H in terms of morphology. The blends filled with 1 wt% of graphene nanoplatelets (Grade C) when compared with neat PS/PMMA blend and the blends filled with 1 wt% of graphene nanoplatelets (Grade H) present a more finer morphology. However, as it can be seen that there is a significant difference in the morphology of the blends with variation in the size of the graphene nanoplatelets used.

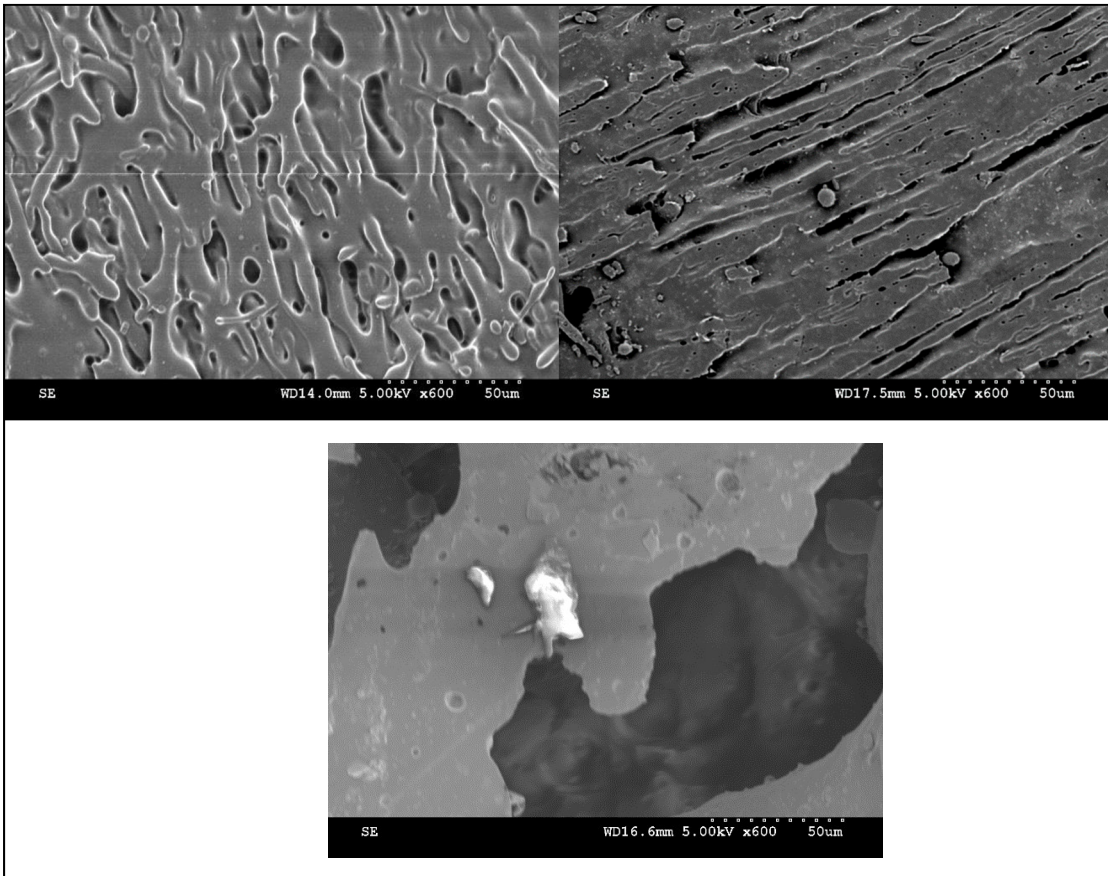


Figure 4.10 Micrographs of a) neat PS/PMMA b)PS/PMMA/Graphene Grade C_PMMA_MB c) PS/PMMA/Graphene Grade H_PMMA_MB samples with ratio of PS/PMMA as 50/50

Thus, from the above observations, it can be suggested that there are various parameters like the masterbatch used, size of graphene nanoplatelets and concentration of graphene nanoplatelets which have significant effects on the characterization of the properties of the blends filled with graphene nanoplatelets. The influence of all these parameters are discussed below.

Influence of the various parameters on the properties of the PS/PMMA/GNPs blends filled with graphene nanoplatelets are as follows:

4.4.1.2. Discussions

4.4.1.2.1. Concentration of the graphene nanoplatelets

From Figure 4.7, it can be observed that there is an increase in the value of conductivity with increase in the concentration of graphene nanoplatelets for all the materials tested in this project but the trend of increase varies for each material. From Figure 4.7, it can also be suggested that as compared to the filled pure polymer phases, the percolation of graphene nanoplatelets for blends starts at a lower concentration than for the filled pure polymer phases. The percolation of graphene nanoplatelets starts at a concentration of 2 wt% of graphene nanoplatelets and it varies for each blend and the highest conductivity value can reach up to 10^{-1} S/m with the filler concentration ranging within just 9 wt% of graphene nanoplatelets. This trend can further be verified by the rheological characterization of the materials.

Rheological characterization is used to estimate the formation of a solid rigid network of the graphene nanoplatelets in the filled blends. From Figure 4.8 and 4.9, it can be observed that there is an increase in the storage modulus with increase in the concentration of graphene nanoplatelets and there is a similarity in the trend of increase in storage modulus at higher frequencies and as observed in the characterization of the electrical properties, the trend is different for different materials. This can be explained by the onset of the formation of the rigid network estimated by the slope analysis of log of storage modulus versus log of angular frequency at lower frequencies. The slope analysis gives an overall view of the formation of solid network which restricts the mobility of the polymer phases.

As can be seen from Table 4.5 and 4.6, the slope of the storage modulus of the filled blends is lower than the slope of the storage modulus of pure polymer phases and the slope decreases with increase in the concentration of the graphene nanoplatelets indicating that the addition of the graphene nanoplatelets helps in restricting the movement of the polymer chains but the trend is different for different materials tested and is dependent on the masterbatch used and size of the graphene nanoplatelets. The influence of these parameters is discussed in the following subsequent sections.

4.4.1.2.2. Masterbatch used

The characterization of the electrical and rheological properties is dependent on the masterbatch used. From Figure 4.7, there is a remarkable difference in the values of conductivity when there is a difference in the masterbatch used. One of the similarities which could be observed in the blends fabricated from different masterbatches is that the values of electrical conductivity increase with increase in concentration but there is significant difference in the value of increment of electrical conductivity or the onset of percolation of graphene nanoplatelets. In case of blends fabricated from PMMA masterbatch, there is a drastic increase in the values of electrical conductivity at a concentration of 2 wt% of graphene nanoplatelets and in case of blends fabricated from PS masterbatch, not much of a significant increase is observed till a concentration of 5 wt% of graphene nanoplatelets but when the concentration of the graphene nanoplatelets is increased from 5 to 9 wt%, the electrical conductivity increases drastically up to a range of 10^{-4} S/m. This fact is further verified by the variation in rheological properties. However, from the figure, it is also clear that the variation in electrical properties also depend on the size of graphene nanoplatelets discussed in the next section.

Rheological characterization results are summarized in Figures 4.8 and 4.9. From the figures, it can be observed that there is a variation in the rheological properties with variation in the masterbatch used. The trend of increase in the storage modulus with angular frequency is similar at higher frequencies for all the materials tested whereas the significant difference is observed at lower frequencies. From Figure 4.9, it can be observed that in case of blends fabricated from PMMA masterbatch, there is a plateau observed at lower frequencies and the storage modulus increases with increase in the concentration of graphene nanoplatelets whereas from Figure 4.8 in case of blends fabricated from PS masterbatch, plateau is observed only at a concentration of 9 wt% of graphene nanoplatelets. This fact suggests the successful formation of the rigid network restricting the mobility of the polymer chains in case of blends from PMMA masterbatch but at a higher concentration of graphene nanoplatelets in case of PS blends. This can be further verified by the slope analysis at lower frequencies indicated in Table 4.5. From Table 4.5 and 4.6, it can be suggested that the decrease in slope of $\log G'$ vs

$\log \omega$ is higher in case of blends fabricated from PMMA masterbatch than the blends fabricated from PS masterbatch suggesting the better dispersion of GNPs in PMMA based blends.

4.4.1.2.3. Size of graphene nanoplatelets

As discussed, the characterization of the electrical and rheological properties of the blends depend on the size of graphene nanoplatelets. From Figures 4.7, 4.8 and 4.9, it can be observed that there is a significant difference in the characterization of electrical and rheological properties of the blends filled with different grades of graphene nanoplatelets provided the masterbatch used for fabrication is same. From Figure 4.7 a), it can be observed that in case of PMMA based blends, there is a remarkable difference in the value of conductivity at a lower concentration of graphene nanoplatelets in the blends filled with graphene grade C and graphene grade H. it can be suggested that in case of the PMMA based blends filled with graphene grade C, the percolation of graphene nanoplatelets start at 2 wt% of graphene nanoplatelets whereas in case of PMMA based blends filled with graphene grade H, no percolation is observed till a concentration of 5 wt% of graphene nanoplatelets and the highest value of conductivity in case of grade C can go up to 10^{-3} S/m whereas in case of grade H, the highest value can go up to 10^{-12} S/m. From Figure 4.7 b), it can be observed that in case of PS based blends, there is not much of a significant difference in the values of conductivity and the highest values of conductivity are in the range of 10^{-14} S/m for the PS based blends filled with graphene grade C and graphene grade H. Hence, it can be suggested that the size of graphene nanoplatelets have a significant influence on the characterization of electrical properties which is further verified by the characterization of rheological properties.

Rheological properties give an estimate of the formation of a rigid solid network. From Figure 4.8 and 4.9, it can be observed that the storage modulus increase with increase in angular frequency and the trend of increase in storage modulus with angular frequency is similar at higher frequencies for all the materials tested. At lower frequencies, the trend is significantly different for blends filled with graphene nanoplatelets of different sizes. From Figure 4.9, it can be observed that a plateau is formed at a concentration of 1 wt% of graphene nanoplatelets in case of blends fabricated from PMMA and filled with graphene grade C whereas a plateau is formed at a concentration of 3 wt% of graphene nanoplatelets in case of blends fabricated

from PMMA and filled with graphene grade H. In case of blends fabricated from PS, no plateau is observed for the blends filled with graphene grade C or grade H. But there is a variation in the trend of increase of storage modulus with increase in the concentration of graphene nanoplatelets for PS based blends filled with graphene grade C or grade H. In case of PS based blends filled with graphene grade C, the increase is gradual whereas in case of blends filled with grade H, the storage modulus at lower frequencies is similar for 1 and 3 wt% of graphene nanoplatelets whereas the increase in storage modulus is steep for 5 wt% of graphene nanoplatelets. From table 4.5, it can be observed that the decrease in slope is less in case of PS based blends filled with grade H as compared to the blends filled with grade C suggesting that the graphene grade C is well dispersed in PS and from Table 4.6, the same observation can be noted for PMMA based blends.

Morphological characterization is used to visualize the microstructure of the blends. The characterization of the morphology of the blends helps in analyzing the microstructure and in supporting the idea of the morphology and the selective localization of the graphene nanoplatelets in the blends supporting the results of electrical and rheological characterization. From Figure 4.10, it can be suggested that the co-continuity of the network prevails in the blends fabricated from PMMA masterbatch irrespective of the filler (Figure 4.10 (b) and Figure 4.10 (c)). Whereas the significant difference in the morphology of the blends fabricated from same masterbatch (PMMA masterbatch) but filled with different grades of graphene nanoplatelets (Graphene Grade C and Graphene Grade H) is that the morphology is refined in the blends filled with Graphene Grade C as compared to the neat blend of PS/PMMA (Figure 4.10 (a)) and the blends filled with Graphene Grade H (Figure 4.10 (b)). The blends fabricated from PMMA masterbatch filled with Graphene Grade H present a more coarse morphology where the size of the continuous phases is large when compared to the phase size of the blends filled with Graphene Grade C. And also from Figure 4.10 (b), in the blends filled with Graphene Grade C, the graphene nanoplatelets can be mostly located at the interface whereas from Figure 4.10 (c), the blends filled with Graphene Grade H, the graphene nanoplatelets can be located in the PMMA phase mostly and some nanoplatelets are found at the interface which suggests that the blends fabricated from PMMA masterbatch and filled with graphene grade C, the graphene nanoplatelets are smaller in size than the graphene grade H and the smaller nanofillers require

less time to migrate towards the interface when compared to the graphene grade H which are larger in size. These blends present a continuous network of graphene nanoplatelets and have lower percolation threshold and higher storage modulus in case of blends filled with graphene grade C when compared to the blends filled with graphene grade H.

Thus, it can be concluded that the percolation threshold is relatively low in case of filled pure blends when compared to the filled pure phases. So, as stated, in order to optimize the cost of the materials, the percolation threshold is optimized as verified by the characterization of electrical and rheological properties and morphological characterization.

4.5. Correlation between the electrical and rheological percolation

The formation of a plateau in G' vs angular frequencies suggest the formation of a rigid GNP network in the system but it does not necessarily indicate a parallel increase in conductivity because rheological percolation generally occurs before the electrical percolation. Even insulating composites which have concentration close to that of the electrical percolation, can still show rheological percolation. This can be clarified by Figure 4.11. Figure 4.11 presents the variation of the storage modulus (G') vs concentration of GNPs for both grades of GNPs in PS and PMMA. From the figure, it can be observed that first remarkable increase of G' occurs for concentration <1 wt% of GNPs having higher surface area (Grade C) for blends prepared from PMMAMB and for concentrations between and 3 wt% of GNPs having lower surface area (Grade H) for blends prepared from PMMAMB whereas increase in electrical conductivity occurs between 1 and 3 wt% of GNPs having higher surface area (Grade C) for blends prepared from PMMAMB and for concentrations between 5 and 9 wt% of GNPs having lower surface area (Grade H) for blends prepared from PMMAMB. Whereas for blends prepared from PSMB, from Figure 4.11, it can be suggested that the first remarkable increase of G' occurs for concentration between 5 and 9 wt% of GNPs having higher surface area (Grade C) as well as for blends prepared from PSMB filled with GNPs having lower surface area (Grade H) The sharp difference in conductivity between the blends filled with different grades of GNPs can be explained by the fact that the aspect ratio of the graphene nanoplatelets affect the stability at the interface and also the migration of the nanoparticles towards the thermodynamically favorable phase. The remarkable difference in the electrical and

rheological behavior for blends prepared from PSMB and PMMAMB can be explained by the mixing sequence.

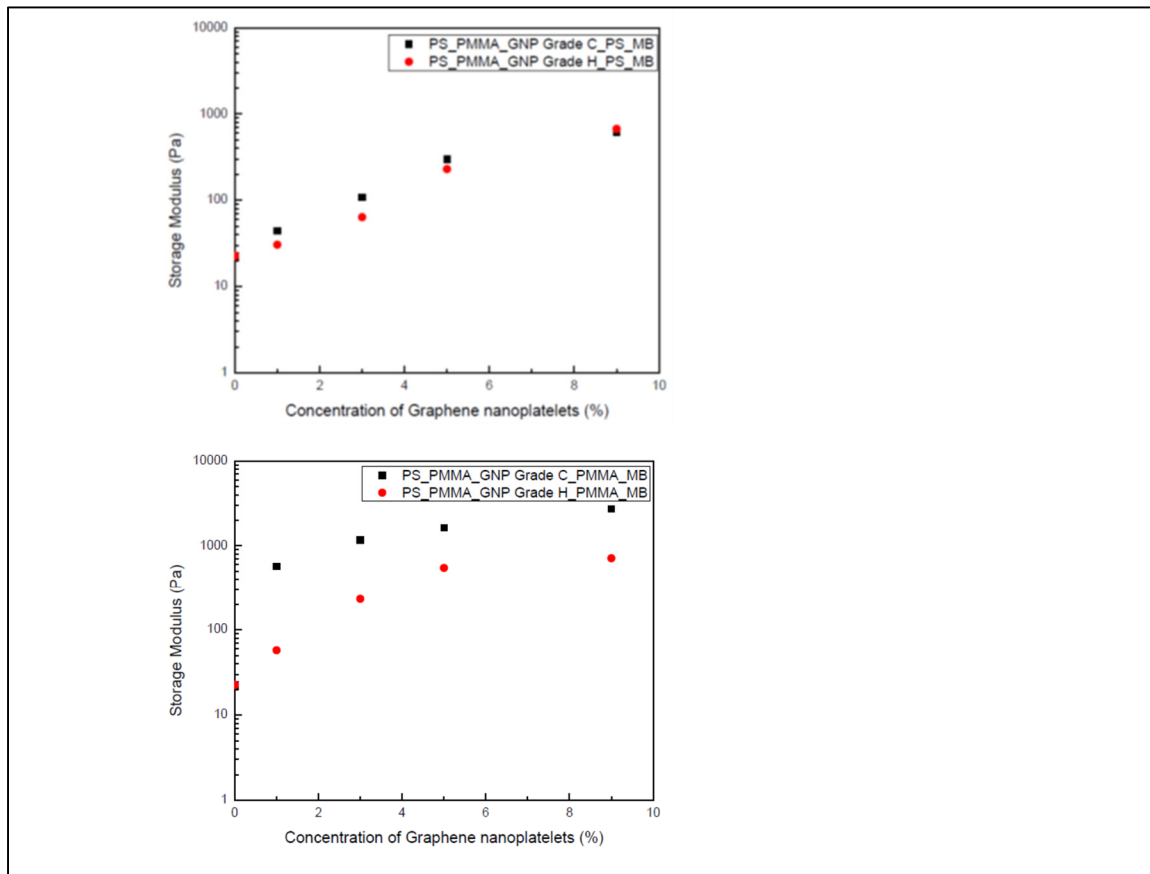


Figure 4.11 Rheological percolation taken at 0.01 rad/s as a function of graphene concentration for different composites prepared from a)PSMB b)PMMAMB

4.6. Effect of annealing on morphology, electrical and rheological properties of the blends

In order to investigate the stability of the PS/PMMA/GNP blends when the graphene nanoplatelets are added, samples of the PS/PMMA/GNPs blends were annealed at 200°C for a time period of 30 minutes, 1 hour and 2 hours. After annealing, the electrical and rheological properties and the morphology was again characterized.

4.6.1. Results

4.6.1.1. Electrical Characterization of annealed blends

Figure 4.12 a) and b) presents the characterization of the electrical properties of the annealed PS based blends with variation in concentration of graphene nanoplatelets. From Figure 4.12a) and b), it can be observed that there is a variation in the trend of increase in the values of electrical conductivity with increase in annealing time for variation in the concentration of the graphene nanoplatelets for PS based blends. From Figure 4.12a), it can also be observed that there is not much of a significant variation in the trend of increase in the value of electrical conductivity with increase in concentration of graphene nanoplatelets (Graphene Grade C) or also with the increase in annealing time for PS based blends when the concentration of graphene nanoplatelets is increased up to 5 wt% of graphene nanoplatelets (Graphene Grade C) but there was a significant increase in the value of electrical conductivity with increase in annealing time when the concentration of the graphene nanoplatelets was increased from 5 wt% to 9 wt% of graphene nanoplatelets and the value of the electrical conductivity remained stable around the range of 10^{-5} S/m for the whole range of annealing time (0 to 120 minutes). From Figure 4.12b), it can be observed that there was not much of a significant variation in the trend of increase in the value of electrical conductivity with increase in concentration of graphene nanoplatelets (Graphene Grade H) when the concentration of graphene nanoplatelets is increased up to 5 wt% of graphene nanoplatelets (Graphene Grade H) but there was a significant increase in the value of electrical conductivity from 10^{-11} S/m to 10^{-5} S/m when the concentration of graphene nanoplatelets was increased from 5 wt% to 9 wt% of graphene nanoplatelets and the value of electrical conductivity remains stable around the range of 10^{-5} S/m for the whole range of annealing time (0 to 120 minutes). Figure 4.12 c) and d) presents the characterization of the electrical properties of the annealed PMMA based blends with variation in concentration of graphene nanoplatelets. From Figure 4.12c) and d), it can be observed that there is a variation in the trend of increase in the values of electrical conductivity with increase in annealing time for variation in the concentration of the graphene nanoplatelets for PMMA based blends when the concentration of the graphene nanoplatelets is increased from 1 wt% to 9 wt%. From Figure 4.12c) and d), it can also be observed that there is a variation

in the trend of increase in electrical conductivity with increase in concentration of graphene nanoplatelets for graphene nanoplatelets of different sizes (increase in conductivity value from 10^{-12} S/m to 10^0 S/m for grade C and from 10^{-14} S/m to 10^{-1} S/m for grade H) and the value of electrical conductivity remains stable around the range of 10^{-1} S/m for a specific range of annealing time (30 to 120 minutes) for the blends filled with graphene grade C or graphene grade H

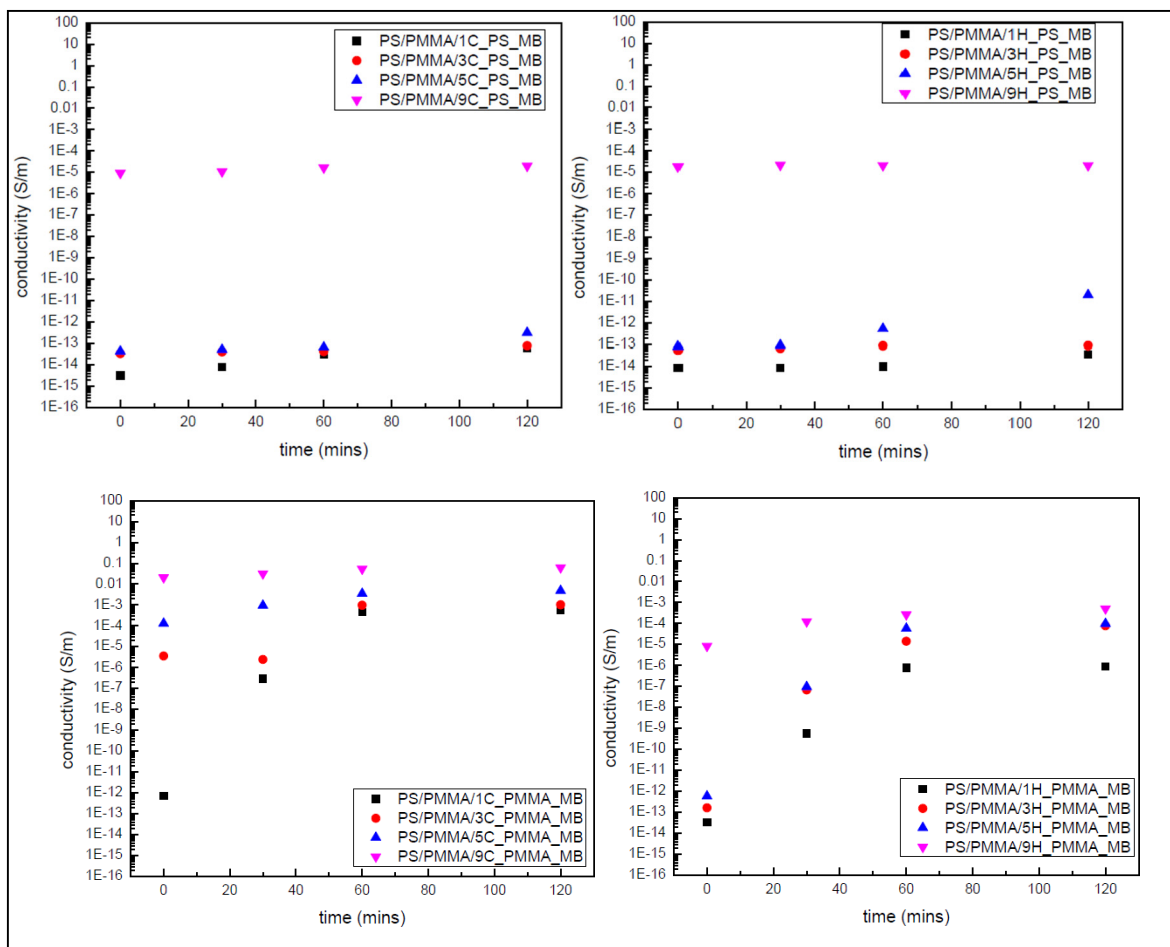


Figure 4.12 Conductivity as a function of concentration of graphene nanoplatelets for annealed blends fabricated from a)PS Masterbatch filled with Graphene Grade C b)PS Masterbatch filled with Graphene Grade H c)PMMA Masterbatch filled with Graphene Grade C d)PMMA Masterbatch filled with Graphene Grade H

4.6.1.2. Time Sweep Tests

Time Sweep Tests were carried on to investigate the rheological properties of the blends annealed at a temperature of 200⁰ C over a time period of 2 hours. Figure 4.13 presents the results of the time sweep tests of the PS based blends filled with graphene grade C and grade H and PMMA based blends filled with graphene grade C and grade H. From Figure 4.13, it can be observed that the storage modulus does not seem to increase over the time period of 2

hours up to a concentration of 5 wt% of graphene nanoplatelets for PS based blends filled with graphene grade C or graphene grade H but with increase in the concentration up to 9 wt% of graphene nanoplatelets, the storage modulus increases over the time being initially and then stabilizes over a time period of 90 minutes for PS based blends filled with graphene Grade C and also for Graphene Grade H. Another fact which can be observed here is that the increase in the storage modulus with time for blends filled with 9 wt% of Graphene Grade C with respect to the lower concentrations of graphene nanoplatelets is smaller when compared to the blends filled with Graphene Grade H. From Figure 4.13, it can be observed that the storage modulus increases over the time being initially and then stabilizes over a time period of 30 minutes for PMMA based blends filled with graphene grade C and over a time period of 65 minutes for PMMA based blends filled with graphene grade H. In case of PMMA based blends, it can be observed that the blends filled with 9 wt% graphene grade C, the storage modulus appears to have reached stability over the whole time period (0 to 120 minutes) whereas in the blends filled with 9 wt% graphene grade H, the storage modulus increases up to 40 minutes followed by stabilization up to 120 minutes.

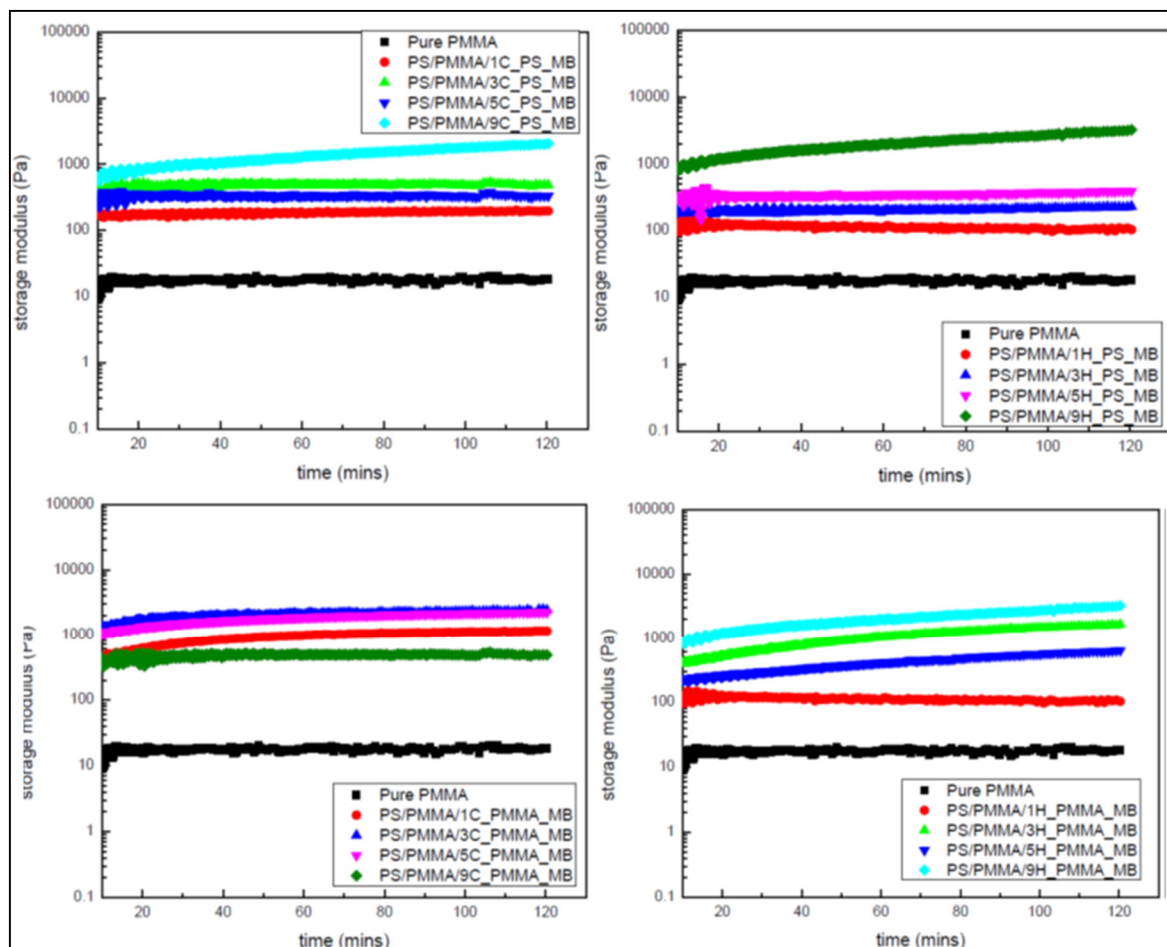


Figure 4.13 Storage modulus as a function of annealing time for blends fabricated from a)PS Masterbatch filled with Graphene Grade C b)PS Masterbatch filled with Graphene Grade H c)PMMA Masterbatch filled with Graphene Grade C d)PMMA Masterbatch filled with Graphene Grade H

4.6.1.3. Morphological Characterization of blends before and after annealing

Figure 4.14 presents the blend morphology of PS/PMMA/GN blends fabricated from PMMA masterbatch (Figure 4.14 a (blends filled with graphene grade C before annealing) and Figure 4.14 b (blends filled with graphene grade C after annealing) Figure 4.14 c (blends filled with graphene grade H before annealing) and Figure 4.14 d (blends filled with graphene grade H after annealing) after being extruded and subjected to compression molding. There is a significant difference in the blends fabricated from PMMA masterbatch filled with graphene grade C before and after annealing and also those fabricated from PMMA masterbatch filled with graphene grade H before and after annealing in terms of morphology. The blends filled

with 1 wt% of graphene nanoplatelets (Grade C) before annealing when compared with the blends filled with 1 wt% of graphene nanoplatelets (Grade C) after annealing and the unannealed blends present a more co-continuous structure than the blends annealed for 60 minutes and the blends annealed for 60 minutes present microstructure with the graphene nanoplatelets which seem to have migrated towards the more favourable phase i.e. PS. But blends filled with 1 wt% of graphene nanoplatelets (Grade H) before annealing and after annealing both present co-continuous morphology. The blends annealed for 60 minutes present a microstructure with the graphene nanoplatelets at the interface. Therefore, it can be suggested that the graphene nanoplatelets having higher surface area migrate faster towards the more favorable polymer phase and accumulate in the more favorable phase. However, as it can be seen that there is a significant difference in the morphology of the blends with variation in the size of the graphene nanoplatelets used and also with thermal annealing.

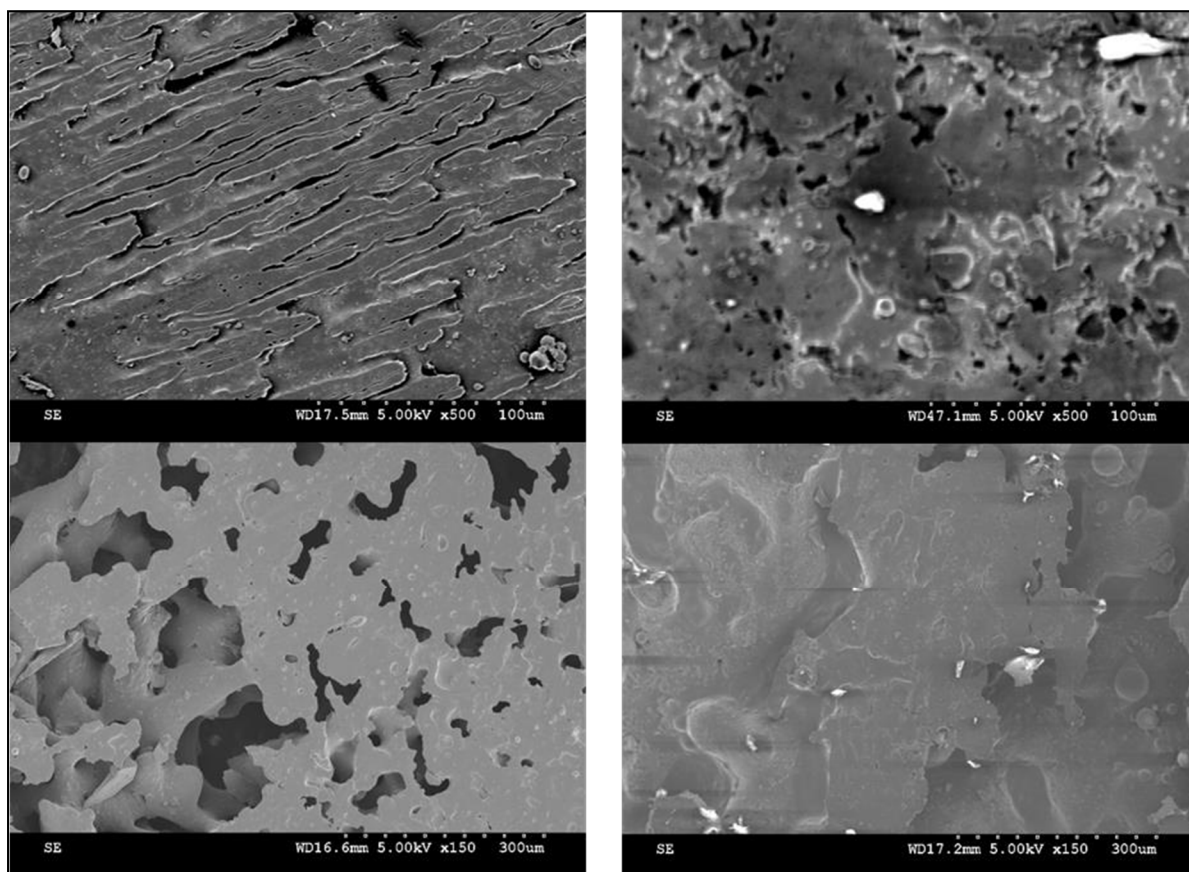


Figure 4.14 Morphology of blends fabricated from a)PMMA Masterbatch filled with Graphene Grade C before annealing b)PMMA Masterbatch filled with Graphene Grade C after annealing c)PMMA Masterbatch filled with Graphene Grade H before annealing d)PMMA Masterbatch filled with Graphene Grade H after annealing for 60 minutes at 200°C.

CONCLUSIONS

In this study, we investigated the co-continuous blends filled with graphene nanoplatelets having different surface areas. It was possible to determine the size effect of the graphene nanoplatelets on the rheological and electrical properties of the blends. Two amorphous polymers Polystyrene (PS) and Polymethylmethacrylate (PMMA) were used as the constituents of the blends and two grades of graphene nanoplatelets having different surface areas were used as fillers. Blends were prepared by melt compounding technique. The electrical conductivity and the rheological characteristics were observed to be dependent on the filler size and also on the filler concentration. The percolation threshold is observed to be lower in case of blends filled with graphene nanoplatelets having higher surface area as compared to the blends filled with graphene nanoplatelets having lower surface area. The conductivity is associated with the formation of a continuous conductive network of graphene nanoplatelets. The migration and rearrangement of the graphene nanoplatelets through thermal annealing is investigated by the trend of rheological characteristics and electrical characteristics. The storage modulus of the materials fabricated from PMMA Masterbatch filled with graphene nanoplatelets having higher surface area evolves during the first 20 minutes followed by stabilization and the storage modulus of the materials fabricated from PMMA masterbatch filled with graphene nanoplatelets having lower surface area evolves during the first 40 minutes followed by stabilization for all concentrations of graphene nanoplatelets except for the materials filled with 1 wt% of graphene nanoplatelets. Whereas on the other hand, the storage modulus of the materials fabricated from PS masterbatch filled with graphene nanoplatelets (irrespective of the grade of graphene) does not have any apparent increase for the whole time range till 5 wt% of graphene nanoplatelets and an increase in the storage modulus is observed when the concentration is increased to 9 wt% of graphene nanoplatelets. On the other hand, the electrical conductivity of the materials fabricated from PMMA masterbatch evolve during the first 60 minutes followed by the stabilization irrespective of the grade of the graphene nanoplatelets and concentration of the graphene nanoplatelets and the electrical conductivity of the materials fabricated from PS masterbatch evolve during the whole time period of annealing irrespective of the grade of the graphene nanoplatelets and concentration of the graphene nanoplatelets. This trend of the electrical and rheological properties of the materials

imply that the materials fabricated from PMMA masterbatch and filled with graphene nanoplatelets having higher surface area have graphene nanoplatelets redistributed to form a co-continuous network faster than the materials filled with the graphene nanoplatelets having lower surface area. Whereas, the trend for materials fabricated from PS masterbatch imply that the redistribution of the graphene nanoplatelets takes a lot of time irrespective of the grade of graphene nanoplatelets.

Therefore, the size of graphene nanoplatelets affect the redistribution of the graphene nanoplatelets in the formation of co-continuous network and strength of the blend matrix

BIBLIOGRAPHY

- ALDRICH. Carbon nanotube, single-walled. In: SIGMA ALDRICH.
- ALDRICH. Copper (II) oxide nanopowder, <50 nm particle size (TEM). In: SIGMA ALDRICH.
- ALDRICH. Graphene nanoplatelets 5 μm particle size, surface area 50-80 m^2/g . In: SIGMA ALDRICH.
- ALDRICH. Graphene nanoplatelets surface area 750 m^2/g . In: SIGMA ALDRICH
- ALDRICH. Silver. In: SIGMA ALDRICH.
- Altobelli, R., de Luna, M. S., & Filippone, G. (2017). Interfacial crowding of nanoplatelets in co-continuous polymer blends: assembly, elasticity and structure of the interfacial nanoparticle network. *Soft Matter*, 13 (37), 6465-6473.
- Ates, M., Karazehir, T., & Sezai Sarac, A. (2012). Conducting polymers and their applications. *Current Physical Chemistry*, 2 (3), 224-240.
- Bai, L., Sharma, R., Cheng, X., & Macosko, C. W. (2018). Kinetic control of graphene localization in co-continuous polymer blends via melt compounding. *Langmuir*, 34 (3), 1073-1083.
- Brigandi, P. J. (2017). *Electrically conductive multiphase polymer blend carbon-based composites*. Lehigh University,
- Brigandi, P. J., Cogen, J. M., & Pearson, R. A. (2014). Electrically conductive multiphase polymer blend carbon-based composites. *Polymer Engineering & Science*, 54 (1), 1-16.
- Canada, G. L. (2015). Graphite vs Graphene. Retrieved from <https://grapheneleaderscanada.com/compare/>
- Cataldi, P., Athanassiou, A., & Bayer, I. S. (2018). Graphene nanoplatelets-based advanced materials and recent progress in sustainable applications. *Applied Sciences*, 8 (9), 1438.
- Chuang, H. K., & Han, C. D. (1984). Rheological behavior of polymer blends. *Journal of applied polymer science*, 29 (6), 2205-2229.
- Database, P. P. (2017). Retrieved from <http://polymerdatabase.com/polymer%20physics/Polymer%20Conductivity.html>

- Dogan, F., Hadavinia, H., J Barton, S., & J Mason, P. (2010). Applications of intrinsically conducting polymers. *Recent Patents on Mechanical Engineering*, 3 (3), 174-182.
- Elias, L., Fenouillot, F., Majesté, J.-C., & Cassagnau, P. (2007). Morphology and rheology of immiscible polymer blends filled with silica nanoparticles. *Polymer*, 48 (20), 6029-6040.
- Fenouillot, F., Cassagnau, P., & Majesté, J.-C. (2009). Uneven distribution of nanoparticles in immiscible fluids: Morphology development in polymer blends. *Polymer*, 50 (6), 1333-1350.
- Filippone, G., Causa, A., Salzano de Luna, M., Sanguigno, L., & Acierno, D. (2014). Assembly of plate-like nanoparticles in immiscible polymer blends – effect of the presence of a preferred liquid–liquid interface. *Soft Matter*, 10 (18), 3183-3191. doi:10.1039/C3SM52995A
- Flagship, G. (2017). The history of graphene. Retrieved from <https://graphene-flagship.eu/material/Pages/The-history-of-graphene.aspx>
- Genoyer, J.(2018). *Compatibilization of PMMA/PS blends by nanoparticles and block copolymers: effect on morphology and interfacial relaxation phenomena* (Doctoral Degree). École de technologie supérieure,
- Hatchett, D. W., & Josowicz, M. (2008). Composites of intrinsically conducting polymers as sensing nanomaterials. *Chemical reviews*, 108 (2), 746-769.
- Helal, E., Kurusu R. S., Moghimian N., Gutierrez, G., David, E., & Demarquette, N. R. (2019). Correlation between morphology, rheological behavior, and electrical behavior of conductive cocontinuous LLDPE/EVA blends containing commercial graphene nanoplatelets. *Journal of Rheology*, 63 (6), 961-976.
- Huang, J. C. (2002). Carbon black filled conducting polymers and polymer blends. *Advances in Polymer Technology: Journal of the Polymer Processing Institute*, 21 (4), 299-313.
- Jeon, H. K., Zhang, J., & Macosko, C. W. (2005). Premade vs. reactively formed compatibilizers for PMMA/PS melt blends. *Polymer*, 46 (26), 12422-12429.
- Koncar, V. (2019). Smart textiles for monitoring and measurement applications. *Smart Textiles for In Situ Monitoring of Composites; Elsevier: Duxford, UK*, 1-151.
- Kozbial, A., Li, Z., Conaway, C., McGinley, R., Dhingra, S., Vahdat, V., . . . Li, L. (2014). Study on the surface energy of graphene by contact angle measurements. *Langmuir*, 30 (28), 8598-8606.

- Kuester, S. (2017). Carbon-based thermoplastic elastomer nanocomposites for electromagnetic interference shielding applications.
- Kumar, R., Singh, S., & Yadav, B. (2015). Conducting polymers: synthesis, properties and applications. *International Advanced Research Journal in Science, Engineering and Technology*, 2 (11), 110-124.
- Lee, J. K., & Han, C. D. (1999). Evolution of polymer blend morphology during compounding in an internal mixer. *Polymer*, 40 (23), 6277-6296.
- Li, J., & Kim, J.-K. (2007). Percolation threshold of conducting polymer composites containing 3D randomly distributed graphite nanoplatelets. *Composites science and technology*, 67 (10), 2114-2120.
- Li, J., Ma, P. L., & Favis, B. D. (2002). The role of the blend interface type on morphology in cocontinuous polymer blends. *Macromolecules*, 35 (6), 2005-2016.
- Li, Y., Lu, D., & Wong, C. (2010). Intrinsically Conducting Polymers (ICPs). In *Electrical Conductive Adhesives with Nanotechnologies* (pp. 361-424): Springer.
- Lin, B., Sundararaj, U., & Guegan, P. (2006). Effect of mixing protocol on compatibilized polymer blend morphology. *Polymer Engineering & Science*, 46 (5), 691-702.
- Liu, X.-Q, Wang, Q.-Y, Bao, R.-Y, Yang, W., Xie, B.-H., & Yang, M.-B. (2014). Suppressing phase retraction and coalescence of co-continuous polymer blends: effect of nanoparticles and particle network. *RSC Advances*, 4 (90), 49429-49441.
- Marsden, A., Papageorgiou, D., Vallés, C., Liscio, A., Palermo, V., Bissett, M., Kinloch, I (2018). Electrical percolation in graphene-polymer composites. *2D Materials*, 5 (3), 032003.
- Materials, A. (2001). Polystyrene- PS. Retrieved from <https://www.azom.com/article.aspx?ArticleID=798>
- Mohan, V. B., Lau, K.-t., Hui, D., & Bhattacharyya, D. (2018). Graphene-based materials and their composites: A review on production, applications and product limitations. *Composites Part B: Engineering*, 142, 200-220.
- Mutlay, İ., & Tudoran, L. B. (2014). Percolation behavior of electrically conductive graphene nanoplatelets/polymer nanocomposites: theory and experiment. *Fullerenes, Nanotubes and Carbon Nanostructures*, 22 (5), 413-433.
- Paul, D., & Barlow, J. (1980). Polymer blends. *Journal of Macromolecular Science—Reviews in Macromolecular Chemistry*, 18 (1), 109-168.

- PLEXIGLAS. PLEXIGLAS 6N. Retrieved from <https://www.plexiglas-polymers.com/en/plexiglas-6n>
- Pötschke, P., & Paul, D. (2003). Formation of co-continuous structures in melt-mixed immiscible polymer blends. *Journal of Macromolecular Science, Part C: Polymer Reviews*, 43 (1), 87-141.
- Ramakrishnan, S. (1997). Conducting polymers. *Resonance*, 2 (11), 48-58.
- Rozik, N. N., Khalaf, A. I., & Ward, A. A. (2016). Studies the behaviors of polyaniline on the properties of PS/PMMA blends. *Proceedings of the Institution of Mechanical Engineers, Part L: Journal of Materials: Design and Applications*, 230 (2), 526-536.
- Salehiyan, R., & Ray, S. S. (2019). Tuning the conductivity of nanocomposites through nanoparticle migration and interface crossing in immiscible polymer blends: A review on fundamental understanding. *Macromolecular Materials and Engineering*, 304 (2), 1800431.
- Scherzer, S. L., Pavlova, E., Esper, J. D., & Starý, Z. (2015). Phase structure, rheology and electrical conductivity of co-continuous polystyrene/polymethylmethacrylate blends filled with carbon black. *Composites science and technology*, 119, 138-147.
- STREM. Graphene Nanoplatelets. Retrieved from https://www.strem.com/uploads/resources/documents/graphene_nanoplatelets_copy1.pdf
- Styrenics, I. Polystyrene Grade Range (PS and PS-I). Retrieved from <https://www.yumpu.com/en/document/read/12987291/polystyrene-grade-range-ps-ps-i>
- Souza, A. M. C. d., Calvao, P. S., & Demarquette, N. R. (2013). Linear viscoelastic behavior of compatibilized PMMA/PP blends. *Journal of applied polymer science*, 129 (3), 1280-1289.
- Taguet, A., Cassagnau, P., & Lopez-Cuesta, J.-M. (2014). Structuration, selective dispersion and compatibilizing effect of (nano) fillers in polymer blends. *Progress in Polymer Science*, 39 (8), 1526-1563.
- Thomas, S., Muller, R., & Abraham, J. (2016). *Rheology and processing of polymer nanocomposites*: John Wiley & Sons.
- Utracki, L. (1999). Polymer blends: fundamentals. In *Polypropylene* (pp. 601-605): Springer.
- Vashishtha, S., Chand, N., & Hashmi, S. (2002). Morphology of PS/PMMA blends and their solution rheology.

- Wang, Y., Shan, J. W., & Weng, G. J. (2015). Percolation threshold and electrical conductivity of graphene-based nanocomposites with filler agglomeration and interfacial tunneling. *Journal of Applied Physics*, *118* (6), 065101.
- Wang, Y., & Weng, G. J. (2018). Electrical conductivity of carbon nanotube-and graphene-based nanocomposites. In *Micromechanics and Nanomechanics of Composite Solids* (pp. 123-156): Springer.
- Willemse, R., Ramaker, E., Van Dam, J., & De Boer, A. P. (1999). Coarsening in molten quiescent polymer blends: The role of the initial morphology. *Polymer Engineering & Science*, *39* (9), 1717-1725.
- You, W., & Yu, W. (2018). Onset reduction and stabilization of cocontinuous morphology in immiscible polymer blends by snowmanlike janus nanoparticles. *Langmuir*, *34* (37), 11092-11100.
- Zhang, C., Zhu, J., Ouyang, M., Ma, C., & Sumita, M. (2009). Conductive network formation and electrical properties of poly (vinylidene fluoride)/multiwalled carbon nanotube composites: Percolation and dynamic percolation. *Journal of applied polymer science*, *114* (3), 1405-1411.
- Ziadan, K. M. (2012). Conducting polymers application. *New polymers for special applications*, 3-24.